Temperature effects on static and dynamic behavior of Consoli Palace in Gubbio, Italy

Alban Kita, Nicola Cavalagli and Filippo Ubertini

University of Perugia, Department of Civil and Environmental Engineering, Via G. Duranti 93, Perugia, Italy

Tel.: +39-075-5853954

Fax: +39-075-5853830

filippo.ubertini@unipg.it (Filippo Ubertini)

Abstract. In recent years, the development of long-term structural health monitoring systems for preventive conservation of historic monumental buildings is receiving a growing trend of scientific interest. Nevertheless, the damage detection effectiveness of these systems is still debated, especially in respect to complex masonry palaces where both local and global failure mechanisms can be activated, whereby the majority of the documented successful applications are limited to masonry towers. In particular, one major issue that needs to be solved in order to derive damage sensitive features is associated to the removal of the effects of changes in environmental conditions and, primarily, of ambient temperature, from static and dynamic signatures. This paper aims to contribute to improving knowledge in this field, by investigating temperature effects on static and dynamic response of an iconic Italian monumental palace: the Consoli Palace in Gubbio. With the purpose of early detecting earthquake-induced damages, as well as damages caused by material degradation associated to awkward environmental conditions, a simple low-cost mixed static and dynamic long-term structural health monitoring system has been installed on the Palace by the authors in July 2017. After discussing surveys, ambient vibration tests, diagnostic investigations, numerical modeling and model calibration of the Palace, the analysis of the first year of monitoring data is presented. This analysis shows that, differently from what observed in other literature works on historic masonry towers, the natural frequencies of the Palace show a marked and sometimes non-linear decreasing trend with increasing ambient temperature, that can be effectively removed through linear statistical filtering provided that dynamic regression models, using past values of predictors, are used. On the other side, the evolution of the amplitudes of two major cracks monitored within the building also shows a marked linear decreasing trend with increasing ambient temperature. These results are meaningful towards the use of monitoring data for assessing the initial health conditions of a structure, as well as in a damage detection perspective.

Keywords. Structural Health Monitoring; Temperature effects; Heritage Preservation; Masonry Buildings; Automated modal identification; FE model updating.

1. Introduction

Masonry structures, such as towers, palaces and churches, constitute the vast majority of Cultural Heritage (CH) buildings in Europe, whose preventive conservation against material degradation and natural hazards is a societal priority, as well as a scientific and technical challenge. Within the Italian context, most of these buildings were built during the Middle Ages and the Renaissance, both in large cities and in small towns, and are especially exposed to the seismic risk, as a consequence of both the high level of seismic hazard of most of Italian territory and of the high seismic vulnerability of such buildings. This has been also dramatically testified by recent Italian earthquakes, such as the ones occurred in Emilia in 2012 [1] and in Central Italy in 2016-2017 [2], just to mention the most recent ones.

Among the various non-invasive diagnostic tools for structural assessment and preventive conservation, ambient vibration tests (AVT) and operational modal analysis (OMA) [3–9], as well as long-term vibration-based structural health monitoring (SHM) [10, 11], are becoming especially popular in application to historic structures, owing to their fully non-destructive and non-invasive nature. In particular, while applications to infrastructure network systems are more traditional [12], literature also counts several applications of vibration-based SHM methods to slender masonry towers

based on the continuous identification of natural frequencies from in-service response data collected by a few sensors deployed on the structure [10, 11, 13-15]. In this context, any damage or change in the structural behavior is automatically detected in the form of anomalies in time series of continuously identified natural frequencies, typically using multivariate statistical analysis methods, while the damage localization task can be addressed by solving an inverse problem, with the purpose to identify damage-induced local changes in equivalent elastic properties of the masonry [16]. While suited for slender structures, vibration-based SHM methods are not directly applicable to stiffer masonry buildings, such as churches and palaces, where a mixed static-dynamic monitoring approach is often more informative, using measurements of strains, deformations, tilts and crack amplitudes to derive static signatures [17-33].

A major challenge in application of SHM systems to historic buildings is represented by the high sensitivity of static (e.g. crack amplitudes) and dynamic (e.g. natural frequencies) signatures of masonry structures to changes in environmental parameters and operational conditions [34]. In particular, temperature is often a dominant driver representing the most important environmental parameter influencing the structural response. However, masonry porosity makes it also sensitive to other environmental conditions and, primarily, to relative humidity and rain affecting moisture content [35-37]. In view of an effective damage detection, the characterization of such environmental effects is crucial for their removal from structural signatures and for the definition of suitable damage-sensitive features. A detailed literature review of temperature effects on static and dynamic signatures, with reference to different typologies of historic masonry structures such as towers and churches, as well as to modern RC structures, deserves to be presented in the following paragraphs.

In the case of slender masonry towers, several authors reported significant changes in natural frequencies caused by temperature fluctuations [10, 11, 13-16, 34-37], often finding an increase in natural frequencies with increasing temperature, conceivably explained as the effect of thermal expansion in the masonry determining closing of superficial cracks or micro-cracks in mortar layers and minor masonry discontinuities (temporary ‘‘compacting’’ of materials induces a temporary increase in structural stiffness) [14, 15, 34, 37]. Similar positive correlations between modal frequencies and temperature were also observed in the case of stiffer masonry structures, such as churches and/or cathedrals [38-40]. It is important to notice that for structures made of different construction materials, such as modern RC structures, negative frequency-temperature correlations were observed. As an example, a recent study on one-year monitoring of an RC beam reported a decrease in modal frequencies with increasing temperature, that was explained as the consequence of a decrease in concrete Young's modulus with increasing temperature [41]. Another notable example concerns long-term monitoring of a whole multi-storey RC building [42], where rather complicated fluctuations of modal frequencies induced by changes in temperature were observed that, most of the times, resulted in decreases in natural frequencies with increasing temperature. In this case, besides the modulus reduction, these effects were explained by also non-uniform temperature distributions leading to support movements and changes in boundary conditions. It can be concluded, therefore, that mechanisms governing temperature effects on modal frequencies can be fundamentally different depending on the type of construction material and on the type of structure under investigation.

Amplitudes of cracks, associated with strains induced by excessive tensile stresses, are also prominently influenced by changes in environmental conditions (e.g. temperature). In general, cracks in masonry structures can be classified as dormant or active [26]. Dormant cracks are mainly due to temporary unstable phenomena (overloading or settlement), while active cracks are usually triggered by damage mechanisms or unstable phenomena and are especially sensitive to changes in environmental conditions that cyclically cause the crack to open and close (breathe). Usually, the crack breathing due to environmental effects has no severe consequences for the structure and the easiest way to detect active cracks is to monitor both their width and growth rate at regular time intervals. The evolution in time of crack amplitudes depends first of all from the heterogeneity and complexity of the structure. Several other factors are crucial such as: crack types, masonry type, boundary conditions, presence of strengthening elements, differential soil settlements and seismic events, just to mention a few. In masonry buildings, both positive and negative correlations with respect to temperature were observed: in the case of relatively stiff historic masonry structures, such as churches, cathedrals and domes, important influence of temperature on static signatures was often observed [27-33], what is also valid for arenas [43], whereas in slender masonry buildings (e.g. towers) a fixed rule is more difficult to be established [44-46].

An effective approach to SHM should include the removal (or minimization) of temperature effects from structural signatures. In order to cope with this issue, some authors proposed to remove the part of variance in signature data associated with changing environmental conditions through the use of proper statistical models, such as multiple data regressions [47] and principal component analysis (PCA) [48-50] and to detect anomalies in the structural behavior by means of statistical process control tools such as control charts [51, 52] revealing very small changes in structural behaviour [15, 53]. This automated detection of small changes in structural performance, typically produced by earthquakes or by other types of dynamic loadings [54, 55], allows a cost-effective management of maintenance and

restoration interventions which is named condition-based maintenance as opposite to breakdown-based or periodic maintenance [56].

In the framework of Horizon 2020 European "HERACLES" project, devoted to enhancing resilience of historic buildings against harmful events, with emphasis on climate-change related effects, a wide research programme was planned in order to develop effective, low-cost SHM methodologies and protocols for application to historic masonry palaces, a structural typology that has been rarely investigated in an SHM perspective. Among the test beds of the project, the Consoli Palace, a monumental middle ages masterpiece of Central Italy located in Gubbio, was chosen as the case study benchmark, because of its notable historic and architectural value, combined with significant evidences of material degradation caused by climate forcing, as well as to a known existing cracking pattern, partly attributable to past seismic events. As an alternative to a dense sensor network [57, 58] that is difficult to be deployed on such a complex masonry building, a simple mixed static and dynamic long-term SHM system was installed by the authors on the Consoli Palace in July 2017 and proposed as a solution for its preventive conservation. To the best of the authors' knowledge, this is the first example in the scientific literature of a stiff masonry Palace being under continuous long-term mixed static-dynamic monitoring with SHM based on natural frequency tracking, whereby the existing literature limits to slender structures such as towers, churches and/or cathedrals, with only sporadic applications of Ambient Vibration Tests to stiffer masonry buildings [59-62]. The simultaneous recording of static and dynamic data have also allowed to improve the statistical model used for the prediction of natural frequencies, by including the crack data as predictors, in addition to temperature data as generally found in literature. By presenting the analysis of the first year of monitoring data, with a focus on the characterization of environmental effects on static and dynamic response of the building, negative frequency-temperature correlations related to a particular crack pattern have been newly observed, alongside with remarkable freezing effects.

The paper is organized as follows. Section 2 presents the case study Palace, including historical background, as well as geometrical and structural damage surveys, highlighting the existing crack pattern. Section 3 presents the results of diagnostic on-site investigations, AVT, OMA, as well as numerical modeling and model calibration. The installation, description and first results of the long-term SHM system are presented and discussed in Section 4, where a specific attention is focused on investigating correlations between natural frequencies and temperature, as well as between amplitudes of major cracks and temperature, including the issue of their statistical reconstruction through dynamic filtering. Finally, Section 5 concludes the paper.

2. The Consoli Palace in Gubbio, Italy

2.1 General overview

The Consoli Palace (Figure 1) is the most representative monument of the medieval town of Gubbio, Italy, and is located in the heart of its historical center. The documentary research indicated that it was designed by Angelo da Orvieto and Matteo Gattapone. Built in gothic style between 1332 and 1349, it hosted the Consuls who were elected to control both legislative and executive branches of the government of the City. Since 1909 the building has hosted the Civic Museum, with a rich collection of art masterpieces, including the Iguvine Tablets dating back to the ancient times of the Umbrian civilization.

With an articulated internal distribution of volumes and an elevation of more than 60 m (from the street level up to the top of the bell-tower), the Palace is built in calcareous stone masonry and has a rectangular plan of about 40x20 m. The building is constituted by bearing walls of relevant thickness and masonry vaults as horizontal elements. The masonry texture is regular and homogeneous. Given the slope of the mountain on which it is erected, the Palace foundations are placed on two different levels: those beneath the "loggia" on the South side are placed approximately 10 m below those beneath the main part of the building. The main façade of the Palace is architecturally characterized by round arched windows in the upper part and merlons above, supported by ogival arches. It overlooks Eastward on the central square of Gubbio, named "Piazza Grande", where the fan-shaped staircase entrance is positioned (Figure 1b). Several restorations were made after 1982 and 1984 earthquakes [63], which were completed in the first half of the 90s. During that period, the façades were completely cleared from accumulations and dirt.

2.2 Geometrical survey and crack pattern analysis

The very first activities carried out on the Consoli Palace consisted of a detailed geometrical survey, on-site material characterization, mapping of material degradation and crack pattern analysis. Material degradation analysis is

not the focus of this work, where, instead, the attention is devoted to those aspects that represent essential information for structural and seismic vulnerability assessment and, primarily, to crack pattern analysis.

Direct observation of the structure was an essential phase of the study to provide an initial understanding of the structure and to properly address the subsequent investigations. In this context, a detailed survey of the building was carried out, including geometrical survey, analysis of materials degradation on the main façades and existing cracking pattern survey. Figure 1 shows two elevations of the building. In particular, East and North façades are shown in Figures 1c and e, respectively. In addition, two sections (parallel to the aforementioned façades) are depicted to highlight the highest and lowest points of the Palace (Figures 1d and f). The loggia constitutes a peculiar architectural portion of the Palace on the South side. The two main halls are the Arengo hall (at height of 4.64 m) and the Nobili hall (at height of 18.89 m).

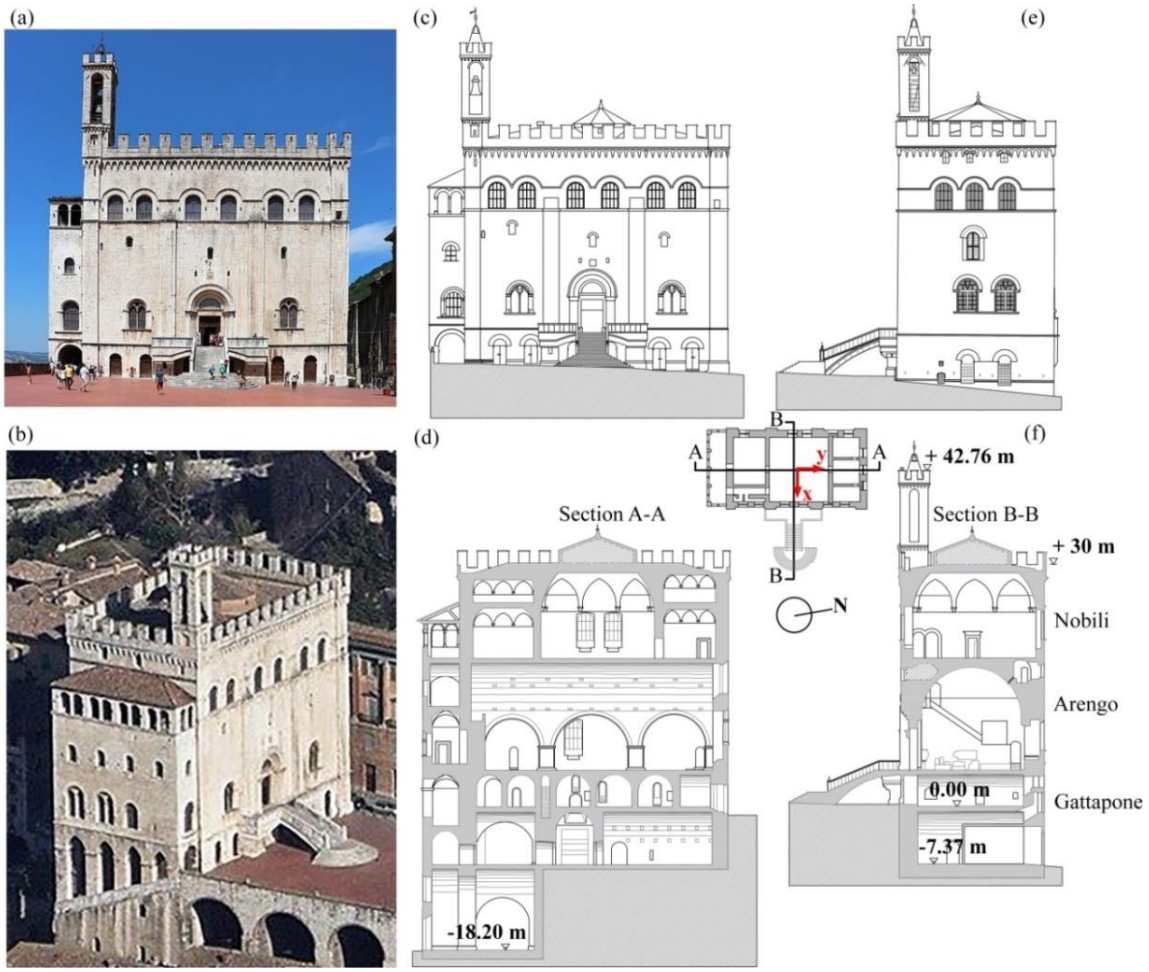

Fig. 1. Front (a) and aerial (b) views of Consoli Palace. Elevation of East (c) and North (e) façades and corresponding sections in the North-South (d) and East-West (f) directions.

Gubbio is located on the Umbria-Marche Apennine Mountains, an area of almost continuous seismic activity that has been defined as a natural laboratory for seismic studies (TABOO – Alto Tiberina Near Fault Observatory). In a range from 1 (high seismicity) to 4 (low seismicity), the area is classified as Zone 2 according to Italian regulations, which is characterized by an average seismicity but where strong earthquakes can occur. Indeed, the city rises on the "fault of Gubbio", a fault well studied by geologists, including subsoil analysis and deep seismological studies [64]. Various strong seismic events have occurred in Gubbio during the last centuries, corresponding to the VIII-X degree of the Mercalli-Cancani-Sieberg macroseismic scale, as documented in macro-seismic catalogues of historic Italian earthquakes. In particular, the Mw5.6 Umbria earthquake occurred on April 29th 1984 [63], with epicentre location between Gubbio and Valfabbrica, caused important damages on the Consoli Palace, as reported by local authorities.

In the context of structural damage analysis, the building pathology was investigated, examining the location (crack mapping), pattern and width of cracks. The Palace exhibits low to moderate structural damage. Figure 2 depicts the major identified cracks with some photo evidence. In general, existing cracks can be the results of the physiological

cracking process of the masonry when subjected to vertical loads. However, it is important to point out that the most important cracks can be related to two possibly activating failure mechanisms and, in particular, to the overturning of the loggia on the South side of the Palace and to the overturning of the northern part of the West façade. The 1st mechanism is highlighted in Figures 2a and b: cracks on the East façade of the Palace are shown in Figure 2a, some of which might be related to the overturing of the loggia, whereas Figure 2b depicts a section of the Palace in the North-South direction (Section A-A) showing the 1st important major crack C1, in correspondence to the junction area between two different types of wall (a stone wall to the left and a brick wall to the right), at the cross-hall leading to the loggia. Microwave tomography-enhanced GPR surveys carried out on Consoli Palace [65] allowed to estimate the depth of the crack as equal to 10 cm, affecting only the first layer of bricks (the thickness of the brick wall is 75 cm). The 2nd mechanism is highlighted in Figure 2c and d: cracks present in the North façade of the Palace are shown in Figure 2c,

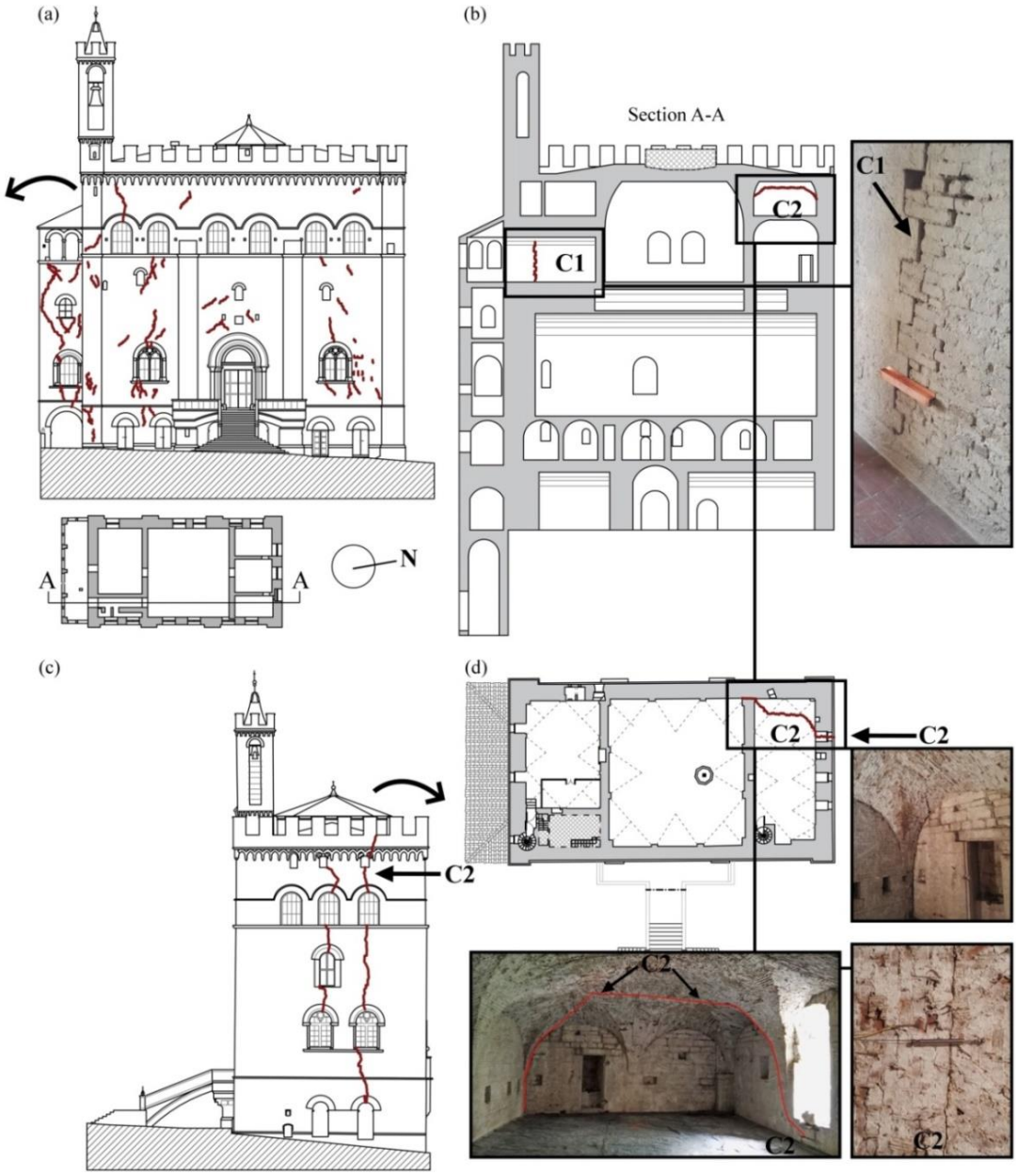

Fig. 2. Structural damage of Consoli Palace: cracks of the East façade showing the possible overturning mechanism of the loggia towards South (a), section A-A of the Palace showing the 1st and the 2nd major cracks, namely C1 and C2, respectively (b), cracks present in the North façade of the Palace where the 2nd major crack C2 is highlighted (c) and plan view of the floor where C2 is present below the vaulted ceiling.

where crack C2 is highlighted; the same crack then proceeds below the vaulted ceiling towards South (Figure 2d) reaching the West façade. These mechanisms might have been activated by past severe events, but could also be partly attributable to differential settlements of the foundations, associated to soil movements during time and to changes in the groundwater

level possibly due to climate-change related effects. On the other hand, widespread cracks scenarios observed in the façades of the building could be related to a combined action of both the stress levels developing inside the material under dead loading and the degradation of the mortar joints, mainly due to environmental actions.

3. On-site investigation and numerical modeling

3.1 Ambient vibration test

An AVT was carried out on the Consoli Palace on May 4th 2017 with the main purpose of evaluating the baseline dynamic characteristics of the building and, in particular, its natural frequencies, mode shapes and damping ratios. This information is crucial for finite element model updating and for designing the continuous dynamic monitoring system, choosing, in particular, the best location for the sensors installed for long-term SHM purposes.

The AVT was conducted on the building using 9 uni-axial high sensitivity piezoelectric accelerometers, model PCB 393B12, capable of measuring accelerations of ±0.50 g with a sensitivity of 10 V/g, g being the gravity acceleration. Sensors were connected to a multi-channel data acquisition system, model NI CompactDAQ-9132, having 24-bit resolution, 102 dB dynamic range and anti-aliasing filters. The tests were conducted in operational conditions, with micro-tremors as the principal source of dynamic excitation, mainly due to wind and weak traffic conditions in the neighbouring roads. Recorded data were collected in separate 30-minutes long files, corresponding to more than 4000 times the fundamental period of the building. The acceleration data were recorded with a sampling frequency of 40 Hz, so to have a Nyquist frequency of 20 Hz, which is safely greater than the largest frequency of interest (10 Hz). Before data processing, a pre-processing procedure has been implemented, in order to remove anomalies (e.g. spikes, etc.) and non-stationary excitation effects produced by the swinging bells, placed in the bell-tower of the Palace, which play with a 15-minutes regularity all day and night long.

During the AVT, accelerometers were deployed on the three main floors of the Palace (at heights of 4.64, 18.89 and 29.77 m, respectively), with a configuration apt to measure rigid diaphragm motions in two orthogonal directions (bending modes), as well as global torsional rotations (Figure 3). Two configuration setups were however considered in order to account for the expected plane deformability of building floors (Figure 3). In the former setup, sensors were deployed close to the short façade of the Palace on the side of the loggia, measuring the motion of the building on its highest side, while in the latter setup they were deployed close to the main façade of the Palace, maximizing the distance between the parallel sensors for better describing global torsional motions.

The level of ambient excitation during the tests was quite low, with measured accelerations not exceeding 0.0015 m/s^2. Two different tools were adopted for extracting the modal parameters from ambient vibration data: (1) the classic Frequency Domain Decomposition (FDD) in its standard and enhanced (EFDD) versions [66], implemented in the commercial ARTeMIS software [67], and an automated technique of Stochastic Subspace Identification (SSI) developed in previous work [5]. As an example regarding application of FDD to recorded accelerations, Figure 4 shows a plot of the first three singular values (SV) of the spectral matrix of the measurements of the second setup. The inspection of this plot has allowed to clearly identify six resonant peaks in the range from 0 to 10 Hz, corresponding to six modes of vibration. As better discussed in the following developments of this work, these modes have been classified on the basis of the identified mode shapes, as well as through the use of a numerical finite element model presented in subsection 3.3. Identified modes have been classified as: two global flexural modes, in *x* and *y* directions, denoted as modes Fx1 and Fy1, respectively, one global torsional mode, denoted as mode T1 and three mixed and/or local modes related to the dynamic interaction between the Palace and the bell-tower and denoted as modes L1, L2 and L3. A possible splitting of the natural frequency of mode L2 is evidenced in Figure 4, whose analysis goes however beyond the purposes of the present study. Table 1 summarizes the estimates of modal parameters in the two setups and considering FDD, EFDD and SSI. These results highlight that the same modes identified through FDD in Figure 4 have been consistently identified in both setups and using all different identification methods, with very similar modal parameters. It is noted that the 2nd configuration resulted in a better agreement between FDD and SSI methods in terms of identified mode shapes, as quantified through Modal Assurance Criterion (MAC) values. Another comment on the obtained results is that identified modal damping ratios are particularly small, which is a consequence of the low levels of ambient vibration during the tests.

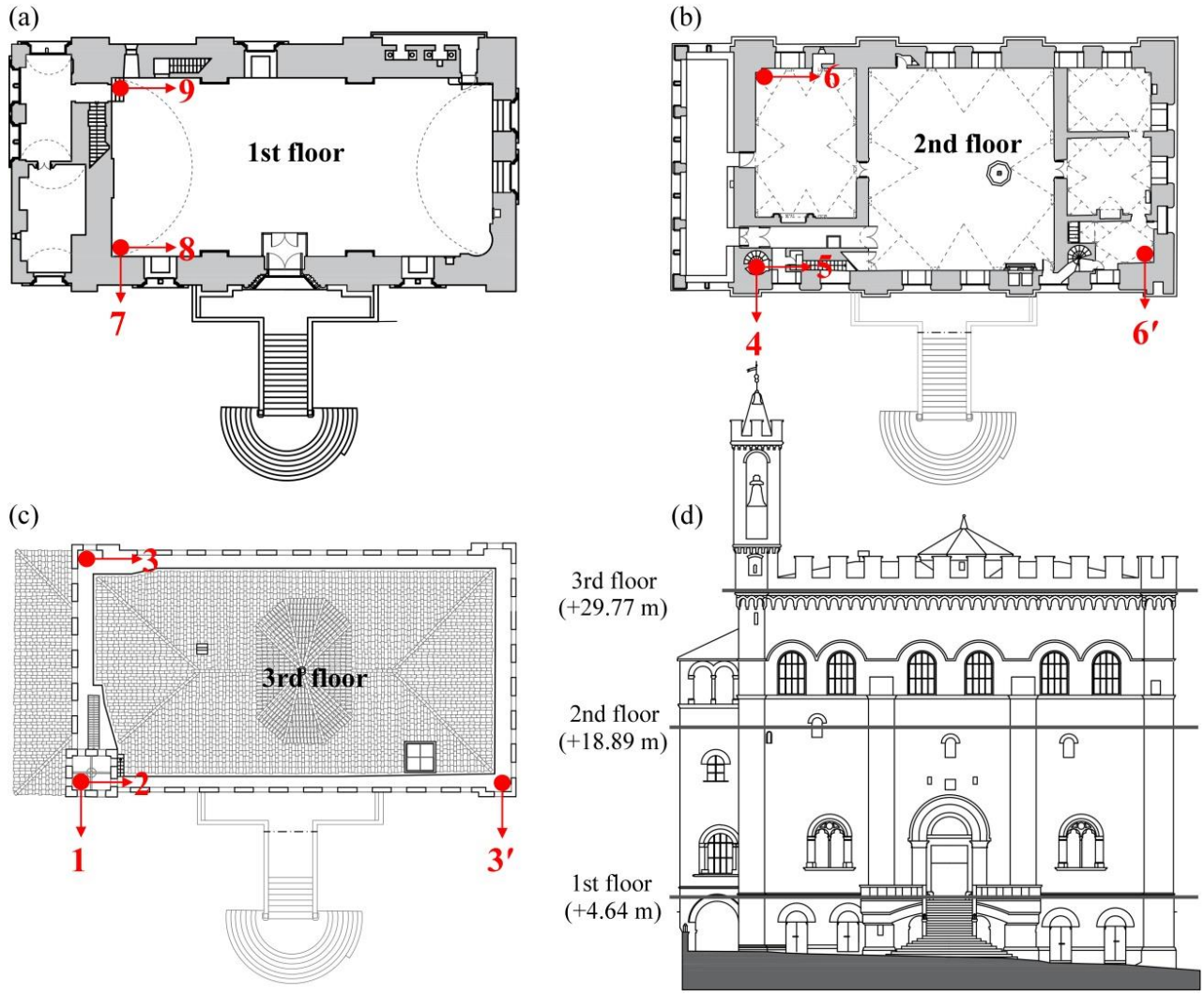

Fig. 3. Sensors layout placed on three floors of Consoli Palace during the AVT of May 4th 2017.

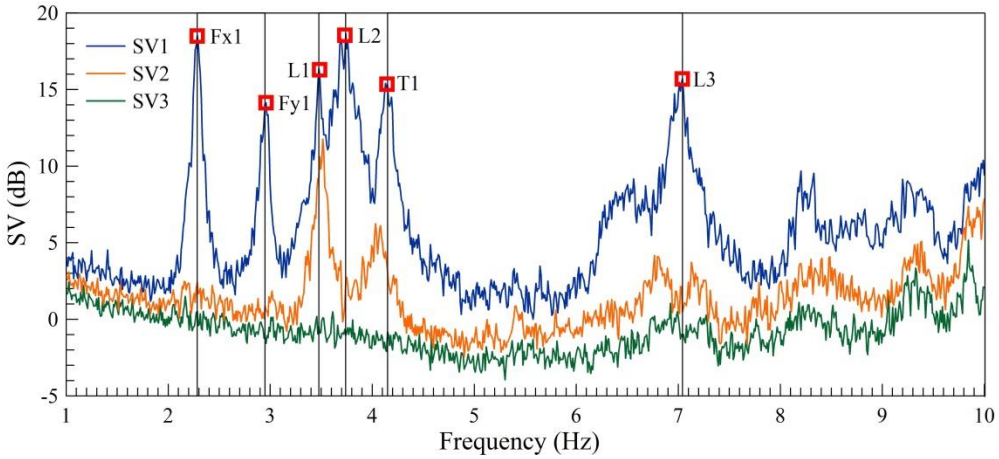

Fig. 4. First three singular values (SV) of spectral matrix of measured accelerations and identified resonant peaks with related modes of vibration.

Identified mode shapes of the three global modes are presented in Figure 5 using the SSI technique and assuming, for the purposes of a better visualization, that the three instrumented floors behave as rigid diaphragms. It should be noted, however, that this hypothesis was not verified through the analysis of recorded accelerations. In this regards, Table 2 summarizes hypothetical rigid modal generalized displacements of the 2nd and 3rd floors, denoted as Δx, Δy and $\Delta\theta$, for the three global modes identified through SSI in the two sensors' configurations. When generalized displacements are remarkably different in the two setups, a modal distortion of the floor is conceivably evidenced. These results allow to

conclude that the 2nd floor behaves as approximately rigid in the two global bending modes, Fx1 and Fy1, while it is not rigid in the case of the torsional mode. On the contrary, in all global modes a distortion of the 3rd floor is highlighted.

Table 1. Identified natural frequencies and damping ratios of the Palace estimated in the 1st and 2nd configuration of AVT (short and main façade, respectively) carried out on May 4th 2017: f_{FDD}, f_{EFDD}, f_{SSI} denote natural frequencies, identified by means of FDD, EFDD and SSI techniques, respectively, whereas ξ_{EFDD} and ξ_{SSI} denote damping ratios estimated with the last two techniques. D_f represents the relative difference in frequency between FDD and SSI, while MAC values are computed between mode shapes as obtained by FDD and SSI techniques, respectively.

Mode	f_{FDD} [Hz]		f_{EFDD} [Hz]		f_{SSI} [Hz]		ξ_{EFDD} (%)		ξ_{SSI} (%)		D_f (%)		MAC	
	Short	Main	Short	Main	Short	Main	Short	Main	Short	Main	Short	Main	Short	Main
Fx1	2.305	2.305	2.297	2.297	2.296	2.296	1.174	1.135	1.092	1.121	0.392	0.392	0.999	0.999
Fy1	2.979	2.979	2.982	2.985	2.990	2.989	0.745	0.999	0.733	0.751	0.368	0.335	0.995	0.988
L1	3.506	3.496	3.507	3.510	3.510	3.508	0.463	0.784	0.752	0.779	0.114	0.342	0.961	0.998
L2	3.721	3.721	3.744	3.741	3.734	3.743	2.456	1.726	2.196	2.477	0.348	0.588	0.998	0.989
T1	4.170	4.170	4.174	4.172	4.172	4.172	1.214	1.431	1.076	1.104	0.048	0.048	0.728	0.999
L3	7.041	7.041	7.049	7.022	7.020	7.035	1.130	0.819	1.142	1.089	0.299	0.085	0.999	0.990

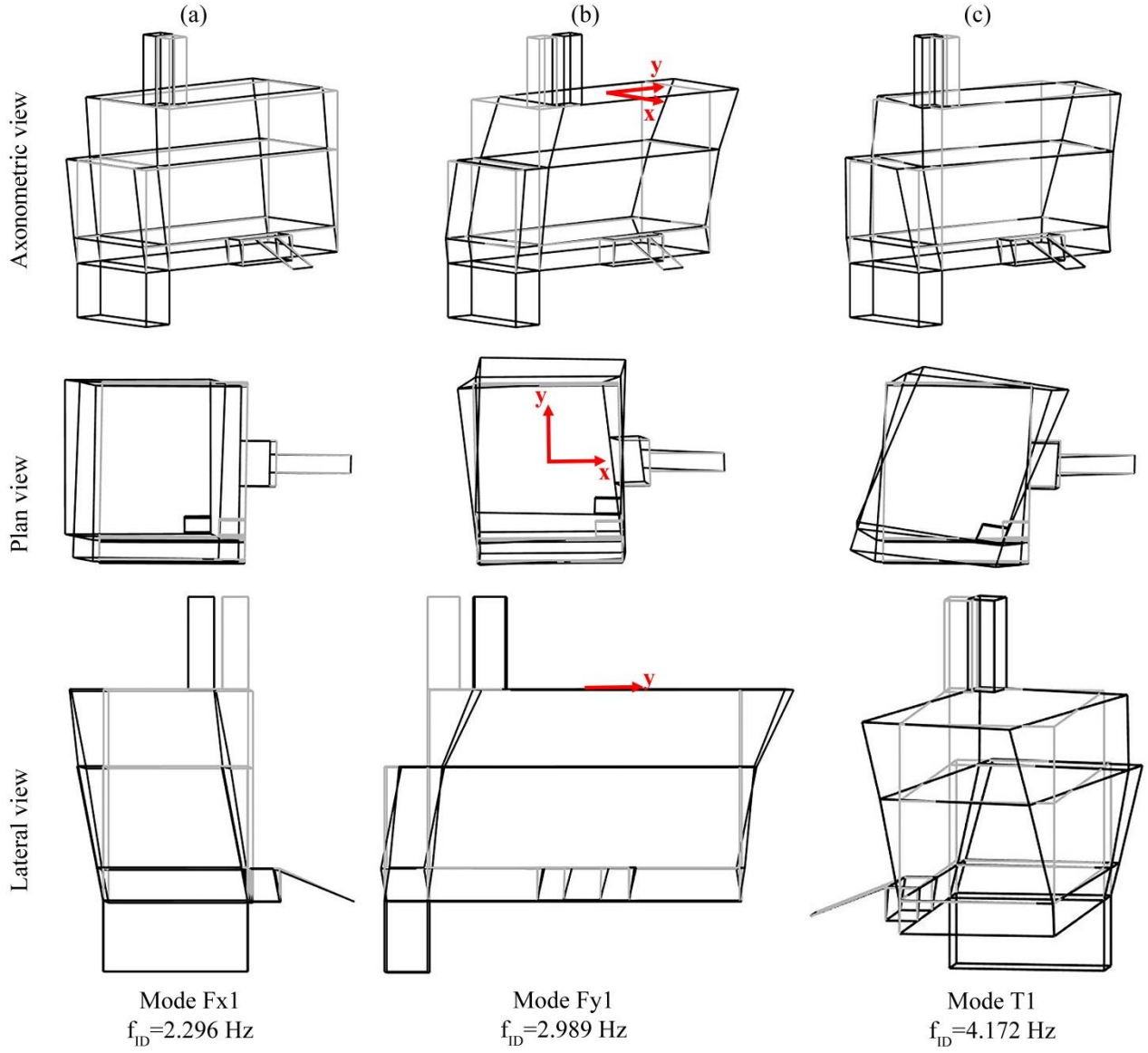

Fig. 5. Global mode shapes of Consoli Palace identified by automated SSI technique. Axonometric, plan and lateral view: flexural modes Fx1 (a) and Fy1 (b) and torsional mode T1.

Table 2. Displacements of each degree of freedom in the plan (Δx, Δy and Δθ) resulting from both configurations (namely short and main) of AVT.

Mode type	Floor	Δx		Δy		Δθ	
		Short	Main	Short	Main	Short	Main
Fx1	2nd floor	1.000	1.000	0.023	-0.058	-0.004	0.004
	3rd floor	1.000	1.000	-0.004	-0.096	-0.011	-0.003
Fy1	2nd floor	0.248	0.296	1.000	1.000	0.001	-0.001
	3rd floor	-0.792	0.104	1.000	1.000	0.040	-0.010
T1	2nd floor	67.201	2.206	20.670	-2.869	1.000	1.000
	3rd floor	48.243	-2.666	14.941	-4.359	1.000	1.000

3.2 Finite element model and model updating

In order to attain a consistent interpretation of the identified local and global modes of vibrations, a 3D numerical model of the structure has been built in the framework of the Finite Element Method (FEM) by using solid hexahedral and tetrahedral elements (see Figure 6a). At the constitutive level, materials have been modeled assuming an isotropic behavior and the non-linear mechanical behavior of masonry has been reproduced, as suggested in relevant literature works [68-70], using the classic concrete damage plasticity model proposed by Lubliner and co-workers [71] and modified by Lee and Fenves [72]. The non-linear constitutive model includes, in particular, both tension and compression damage. However, in this paper only the elastic behaviour of the Palace is considered, while the characterization of the parameters of the damage model goes beyond the purpose of the present investigation.

Based on the architectural survey (Figure 1), the model has been subdivided in four nominally homogenous parts: the Gattapone level, the Arengo level, the Nobili level and the bell-tower. In order to account for possible differences in material properties in such portions of the building, these parts have been assigned different values of the Young's modulus of the masonry. On the contrary, the same value of Poisson's coefficient, ν, and of material density, ρ, have been considered in the whole building. Young's moduli of materials in the four homogeneous regions of the building, Poisson's coefficient and material density have been treated as uncertain parameters and their values have been calibrated in such a way to minimize the average relative difference between numerically predicted and experimentally identified natural frequencies of vibration. Overall, the availability of six identified vibration modes ensures that the inverse problem, consisting of the calibration of six uncertain parameters, is well-posed.

Model tuning has been performed in three steps. First of all, initial guess values have been assigned to all uncertain parameters using values suggested in the Italian technical standard code (step NTC 2008) [73]. In a second step, Young's moduli have been corrected using values estimated from sonic pulse velocity tests, as simple and fully non-invasive diagnostic investigations [35, 74] (step called NTC 2008+Sonic). Tests were carried out in both direct and indirect (or superficial) configurations. Values of measured elastic compression and surface Rayleigh wave velocities enabled an average estimation of the Young's modulus, E=3327 N/mm^2, and Poisson's ratio, υ=0.34, of on-site masonry [75], under the assumption that it behaves as an elastic and homogeneous material. The 3rd and final step (step called Calibration) consisted of a one-step manual tuning. Accordingly, the FEM model has been used to construct the following approximate linear relationship between the vector of estimated natural frequencies, $\boldsymbol{f}_{\mathrm{FEM}}$, and the vector of uncertain parameters, $\mathbf{X}$:

$$\boldsymbol{f}_{\mathrm{FEM}} \cong \boldsymbol{f}_{0,\mathrm{FEM}} + \mathbf{S}(\mathbf{X} - \mathbf{X}_0) \quad (1)$$

where $\mathbf{X}_0$ contains initial guess values of the aforementioned six uncertain parameters and $\boldsymbol{f}_{0,\mathrm{FEM}}$ the corresponding natural frequencies, while $\mathbf{S}$ is a matrix containing sensitivity coefficients of natural frequencies with respect to changes in model parameters that have been estimated through a series of numerical modal analysis considering small variations of such parameters one at a time. Then, the vector containing updated values of uncertain parameters, $\mathbf{X}_1$, has been estimated as:

$$\mathbf{X}_1 = \mathbf{X}_0 + (\mathbf{S}^{\mathrm{T}}\mathbf{S})^{-1}\mathbf{S}^{\mathrm{T}}(\boldsymbol{f}_{\mathrm{ID}} - \boldsymbol{f}_{0,\mathrm{FEM}}) \quad (2)$$

where $\boldsymbol{f}_{\mathrm{ID}}$ is a vector containing identified values of natural frequencies.

Table 3 summarizes values of uncertain parameters in the three tuning steps, while target and numerically predicted natural frequencies of vibration are summarized in Table 4. Table 4 also compares experimental (as estimated by FDD method) and numerical mode shapes of global modes by means of MAC values. Overall, a very good consistency is evidenced between the real structure and the FE model after the third step, with an average relative deviation in natural frequencies, Δf_{mean}, equal to 1.818 %. Even though modal shapes were not considered in model

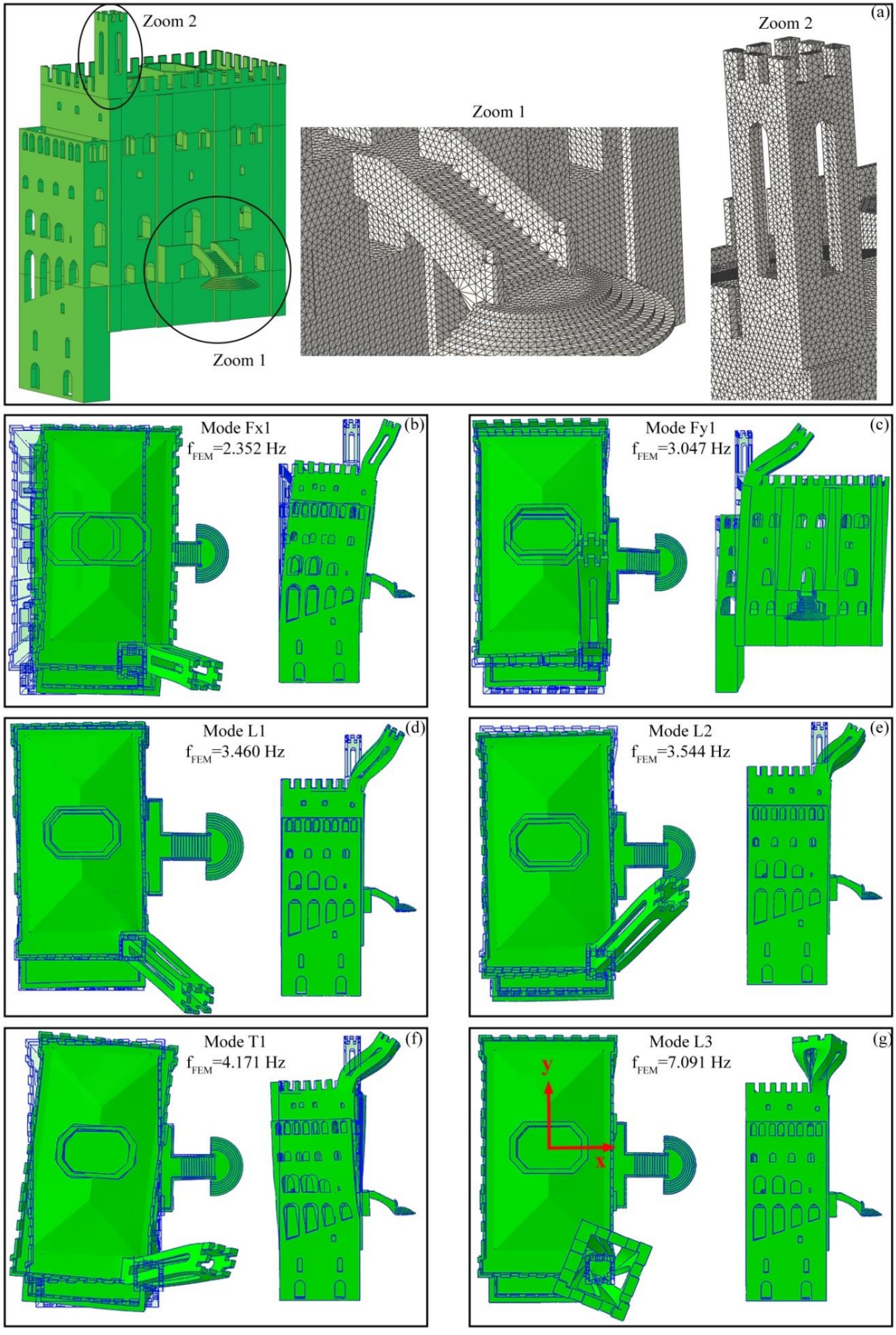

Fig. 6. Numerical model of Consoli Palace (a): general view and detailed view of finite element discretization of the bell-tower and the fan-shaped staircase entrance. First six mode shapes of Consoli Palace predicted using the calibrated numerical model: global modes Fx1, Fy1 and T1 (b, c and f, respectively) and local modes L1, L2 and L3 (d, e and g, respectively).

calibration, relatively high MAC values (higher than 0.96) are observed for two global modes (Fx1 and T1), whereas a relatively poorer quality of model calibration has been observed for the mode shape of mode Fy1 (MAC value equal to 0.74). Overall, this result is believed to be affected by the imperfect capability of the numerical model in capturing the global distortion of the building that is partly attributable to the existing damage pattern that has not been included in the numerical model for the sake of simplicity. This aspect is however considered as marginal in the context of the present study and the achieved model calibration is therefore regarded as sufficiently accurate for the purposes of the present investigation. Figure 6 also depicts the FE-predicted mode shapes of the Consoli Palace after model tuning. These results confirm the global nature of modes Fx1, Fy1 and T1, as well as the local nature of modes L1, L2 and L3. In particular, Fx1 is confirmed to be a flexural mode along the x direction (East-West direction), Fy1 a flexural mode along the y direction (North-South direction) and T1 a torsional mode. Local modes L1, L2 and L3, mostly affect the bell-tower with slight but measurable movements on top of the building: L1 and L2 are flexural modes of the tower, whereas L3 is a torsional one.

Table 3. Parameters assumed in the FE numerical model of Consoli Palace in the three steps of model calibration.

Part	Parameter	NTC2008	NTC2008+Sonic	Calibration
Gattapone level	E_1 [N/mm^2]	2440	3327	3327
Arengo level	E_2 [N/mm^2]	2440	3327	3510
Nobili level	E_3 [N/mm^2]	2440	3327	3327
Bell-tower	E_4 [N/mm^2]	2440	3327	3450
All	ν	0.20	0.34	0.34
All	ρ [t/m^3]	1.90	1.90	1.90

Table 4. Comparison between experimentally identified (f_{ID}) by FDD technique and numerically predicted natural frequencies (f_{FEM}), where Δf represents the relative difference and Δf_{mean} the mean relative difference.

	Exp.	NTC2008			NTC2008+Sonic			Calibration		
Mode	f_{ID} [Hz]	f_{FEM} [Hz]	Δf (%)	MAC	f_{FEM} [Hz]	Δf (%)	MAC	f_{FEM} [Hz]	Δf (%)	MAC
Fx1	2.305	1.991	13.623	0.987	2.326	0.911	0.986	2.352	2.048	0.988
Fy1	2.979	2.586	13.192	0.761	3.012	1.108	0.739	3.047	2.299	0.738
L1	3.496	2.920	16.476	-	3.413	2.374	-	3.460	1.047	-
L2	3.721	2.994	19.538	-	3.495	6.074	-	3.544	4.773	-
T1	4.170	3.599	13.693	0.972	4.123	1.127	0.971	4.171	0.029	0.967
L3	7.041	6.025	14.430	-	6.965	1.079	-	7.091	0.713	-
		Δf_{mean} =15.159 %			Δf_{mean} =2.112 %			Δf_{mean} =1.818 %		

4. Long-term structural health monitoring

4.1 The monitoring system

All previously described activities have guided the installation of a simple and low-cost mixed static-dynamic long-term SHM system on the Consoli Palace, that has been continuously recording since July 2017. The main purpose of this SHM system is the early detection of damage-induced anomalies in the time series of the amplitudes of the two major cracks existing in the building and related to possible failure mechanisms (see Subsection 2.2), as well as in the time series of the natural frequencies of global and local vibration modes.

The SHM system comprises: three accelerometers, two crack meters, two temperature sensors and one data acquisition system with remote connection to a data analysis server located in the Laboratory of Structural Dynamics of University of Perugia. The layout of the system is illustrated in Figure 7. For the purpose of natural frequency identification and tracking, three high sensitivity uni-axial piezoelectric accelerometers model PCB 393B12 (10 V/g

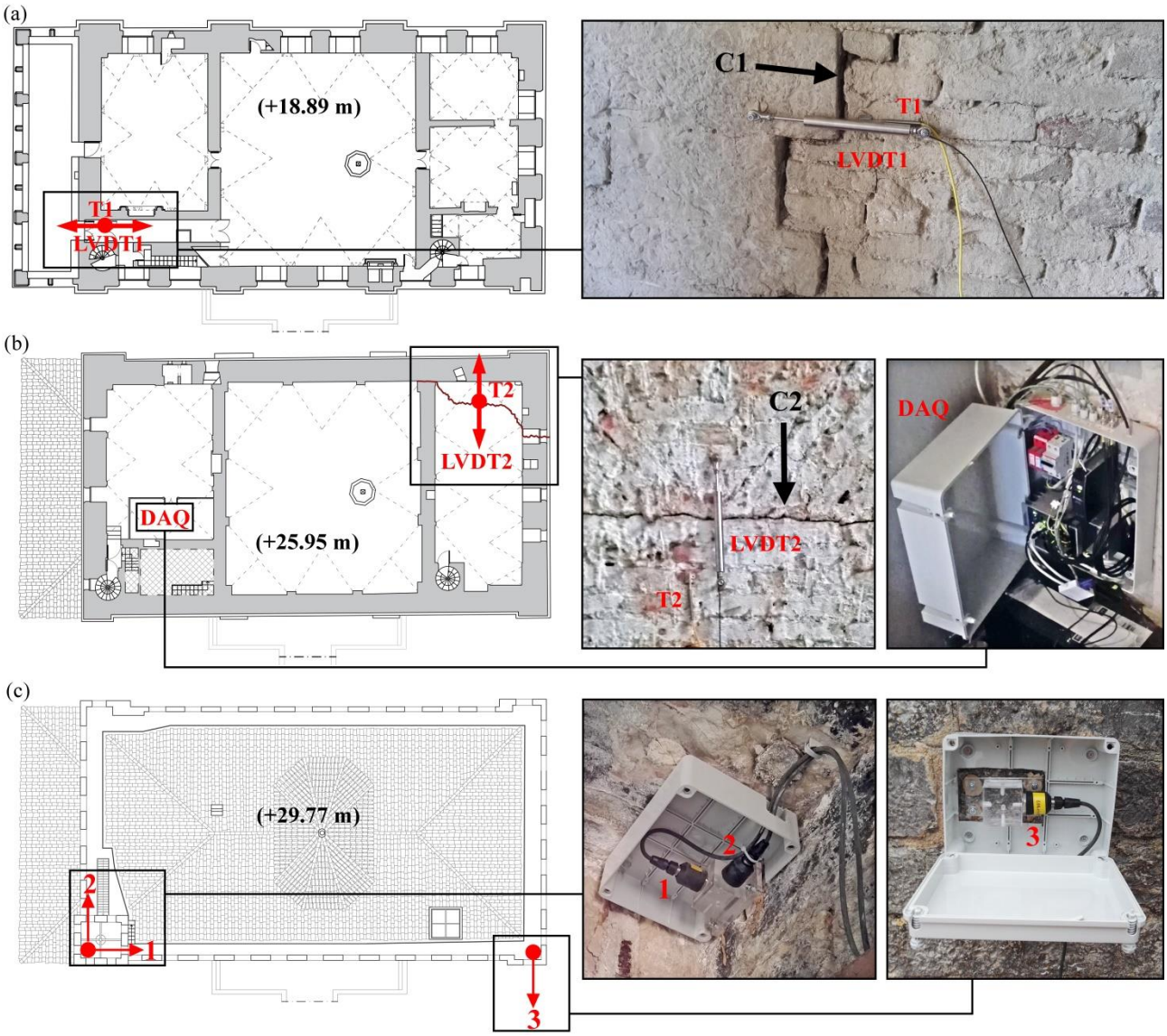

Fig. 7. Long-term static-dynamic SHM system installed on the Consoli Palace: LVDTs and temperature sensors' layout with detailed view of positioning in correspondence of the 1st and 2nd main crack ((a) and (b), respectively, where the double arrows indicate the direction of opening of the monitored crack) and accelerometers locations (c).

sensitivity and ± 0.5 g measuring range) have been deployed on the roof of the Palace, with a configuration that allows to observe all modes of interest, including both global and local ones. In addition to the three accelerometers, two crack meter sensors have also been permanently installed across cracks C1 and C2, controlling the possible occurrence of unstable phenomena. Two Linear Variable Displacement Transducers (LVDT), S-Series model with measurement range from 0 to 50 mm and resolution <0.3μm, are used for this purpose. Two K-type thermocouples (denoted as T) are also installed close to each LVDT, in order to measure the surface temperature of the wall aiming at observing its influence on the evolution of the cracking pattern, as well as on global vibration modal properties.LVDT1 and T1 are installed in the South part of the Palace, in correspondence to the main bearing wall, in order to measure the amplitude of crack C1, whereas LVDT2 and T2 are placed across crack C2 on the vaulted ceiling close the North façade (the crack on the main bearing wall of the North façade proceeds inwards on the vaulted ceiling). Data outputted by all sensors are recorded by using a data acquisition system, model NI CompactDAQ-9132, supplied through an Uninterruptible Power Supply (UPS), with the following technical characteristics: processor 1.33 GHz Dual-Core Atom, 2 GB RAM, 16 GB SD storage, 4-Slot, Windows Embedded Standard 7 operating system. The data acquisition system mounts one NI 9234 acceleration acquisition module (24-bit resolution, 102-dB dynamic range, and anti-aliasing filters) and one NI 9219 crack amplitude and temperature acquisition module (24-bit resolution, ±60V range, 100S/s). A LabVIEW toolkit is implemented [76] and used for data acquisition and preliminary real-time processing, such as amplitude and spectral plots, that are used for quality control of the data from remote. Data are stored in consecutive separate files containing 30 minute recordings.

Accelerations are sampled at 100 Hz, while crack amplitudes and temperature values are sampled at 0.1 Hz. The recorded data are then sent through the Internet to the remote server, where they are processed through an ad hoc developed MATLAB code, using each stored 30-minute-long recording file for automated modal analysis and anomaly detection. The data processing code comprises the following steps: (1) decimation of the data to 40 Hz after application of an anti-aliasing low-pass filter with delay compensation; (2) pre-processing analysis with de-trending and de-spiking of the raw-data and also correcting other anomalies in the data, in particular, eliminating non stationary excitations from swinging bells that play with a 15 minute regularity; (3) application of the fully automated SSI modal identification procedure developed in [5]; (4) modal tracking based on a similarity check between estimated modal parameters and (5) application of a multivariate statistical tool for removing environmental effects from times series of natural frequencies and crack amplitudes and for detecting damage-induced anomalies in the data. Data reported in this paper refer to the first four steps of the procedure and cover a continuous monitoring period of one year, considering the time span starting from July 5th 2017, date of activation of the monitoring system, up to July 5th 2018.

4.2 Monitoring data analysis

The recorded time series of crack amplitudes are plotted in Figure 8 and some statistical information are summarized in Table 5, considering the one year monitoring period. Time histories are available with a sampling time of 30 minutes, with occasional short interruptions due to lightning shocks hitting the building during storms. The analysis of monitoring data highlights that cracks C1 and C2 exhibit similar amplitude changes, ranging between a closing of 0.07 mm to an opening of 0.3 mm. The two cracks also exhibit very similar seasonal trends, with closing in summer and opening in winter. Apparent daily fluctuations of crack amplitudes are also evidenced with a detailed view. Overall, a clear temperature driven crack breathing is therefore highlighted from the presented results, that will be further discussed in the following developments of this work.

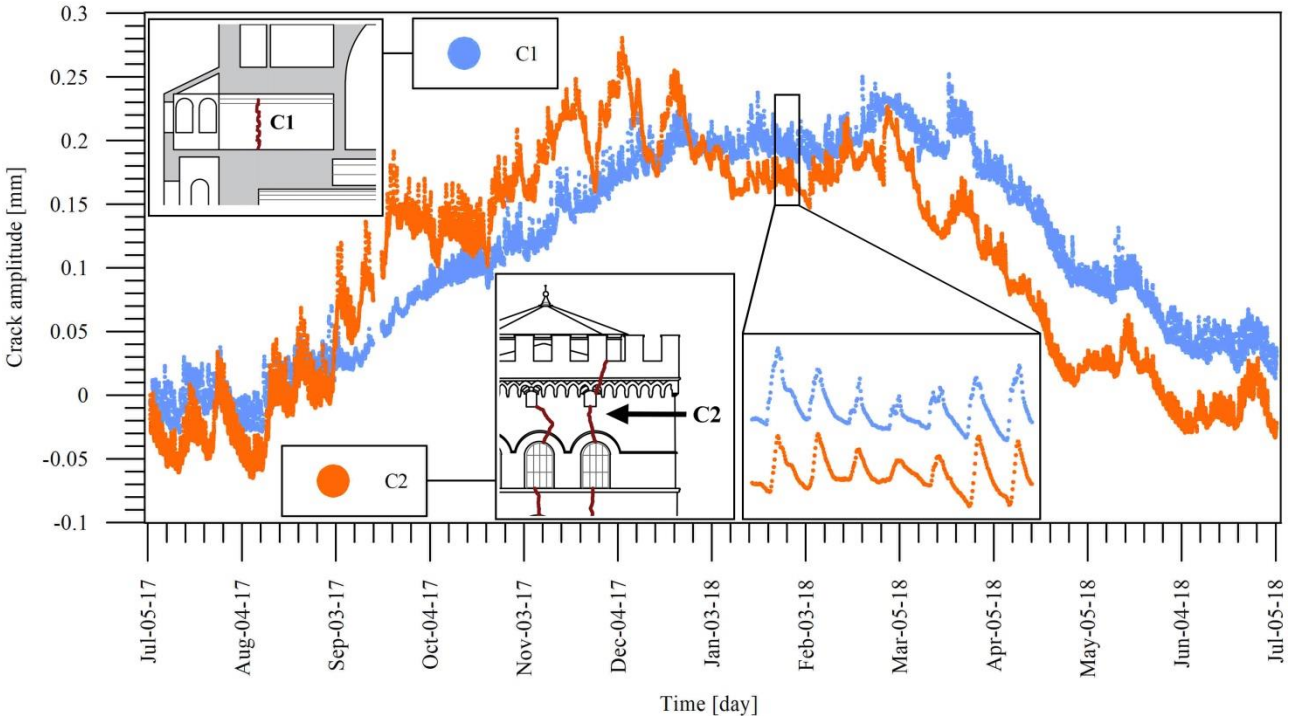

Fig. 8. Evolution in time of two monitored crack amplitudes of Consoli Palace during the first year of monitoring.

Results of continuous modal identification and frequency tracking are presented in Figure 9 and synthesized with some statistical information in Table 5. These results show that modal tracking is possible for all natural frequencies of the six vibration modes identified through the AVT presented in Subsection 3.1, though some natural frequencies are consistently identified in a larger number of data sets, conceivably due to comparatively larger excitation levels of some modes. In particular, modes Fy1 and L2 exhibit lower identification success ratios, which might be associated to a lower traffic excitation during night hours, but they can still be tracked with an acceptable continuity. Overall, the presented

results show clear seasonal variations and apparent daily fluctuations of the natural frequencies of some modes, variation which is discussed and investigated in the next section.

Table 5. Statistics of measured crack amplitudes and temperature data and identified natural frequencies from July 5th 2017 to July 5th 2018 (x_{ave} denotes the mean value, σ_x the standard deviation, CV the coefficient of variation, x_{min} and x_{max} the extreme values and ID success ratio the relative frequency of consistently identified natural frequencies of a specific mode and/or recorded crack amplitudes and temperature).

Crack	C_{ave} [mm]	σ_c [mm]	CV [%]	C_{min} [mm]	C_{max} [mm]	ID success ratio (%)
C1	0.110	0.075	0.681	-0.029	0.252	100
C2	0.097	0.089	0.920	-0.065	0.281	100
Mode	f_{ave} [Hz]	σ_f [Hz]	CV [%]	f_{min} [Hz]	f_{max} [Hz]	ID success ratio (%)
Fx1	2.309	0.022	0.010	2.252	2.387	95.31
Fy1	2.962	0.093	0.032	2.720	3.246	58.22
L1	3.474	0.069	0.020	3.234	3.683	80.77
L2	3.748	0.036	0.010	3.597	4.084	47.96
T1	4.167	0.057	0.014	3.945	4.463	94.05
L3	7.036	0.111	0.016	6.621	7.354	64.01
Temp	T_{ave} [° C]	σ_T [° C]	CV [%]	T_{min} [° C]	T_{max} [° C]	ID success ratio (%)
T1	18.546	7.212	0.389	3.730	34.118	100
T2	17.167	8.037	0.468	5.397	31.128	100

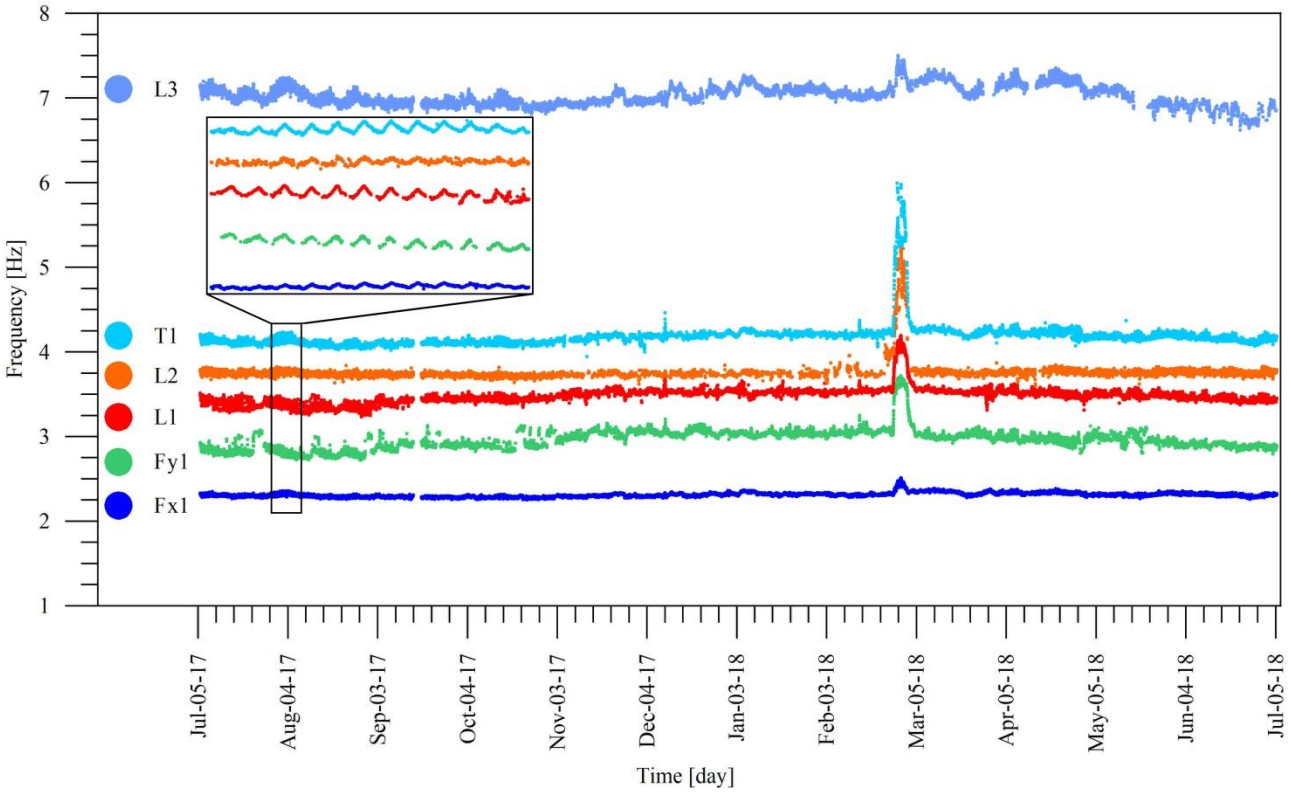

Fig. 9. Time series of identified natural frequencies of Consoli Palace using automated SSI during the first year of monitoring.

4.3 Temperature effects: correlation analysis

Temperature effects on crack amplitudes and natural frequencies of the Consoli Palace are investigated in this section considering the same time period investigated above, while a specific attention will be devoted in the following developments of the work to the time period from February 26th to March 1st when exceptional freezing conditions occurred.

Table 5 also summarizes some statistical information regarding the measured temperature data, highlighting that the observed temperature range goes from 3.7 °C to 34.1 °C. In general, since sensor T1 is almost located outdoor, it shows more significant daily temperature fluctuations compared to sensor T2 that is located indoor. Correlation

coefficients between temperature data are summarized in Table 6, showing that the two temperatures are highly correlated. Table 6 also summarizes correlation coefficients between crack amplitudes and temperature data. These results show an overall large degree of correlation, with negative correlation coefficient values larger than 0.78. This negative correlation is visually highlighted in Figure 10 where it is shown that the amplitude of crack C1 is almost perfectly linearly correlated with temperature T1 (plot of the amplitude of crack C1 is almost overlapped to temperature data measured by sensor T1 taken with a negative sign), while some shift between temperature T2 and amplitude of crack C2 is evidenced, conceivably due to the thermal capacity of the masonry. Overall, it is confirmed that crack amplitudes are largely dominated by temperature changes. In particular, decreasing temperatures cause a global contraction of structural masonry volumes, resulting in opening of cracks C1 and C2. On the contrary, increasing temperatures result in crack closing.

Table 6. Correlation coefficients between temperatures, crack amplitudes and natural frequencies in the monitoring period.

	T1	T2	Fx1	Fy1	L1	L2	T1	L3
T1	1.000	0.990	-0.414	-0.846	-0.831	-0.172	-0.713	-0.382
T2	0.990	1.000	-0.420	-0.854	-0.840	-0.173	-0.717	-0.400
C1	-0.980	-0.986	0.371	0.843	0.815	0.124	0.678	0.379
C2	-0.789	-0.829	0.017	0.794	0.659	0.068	0.359	0.009

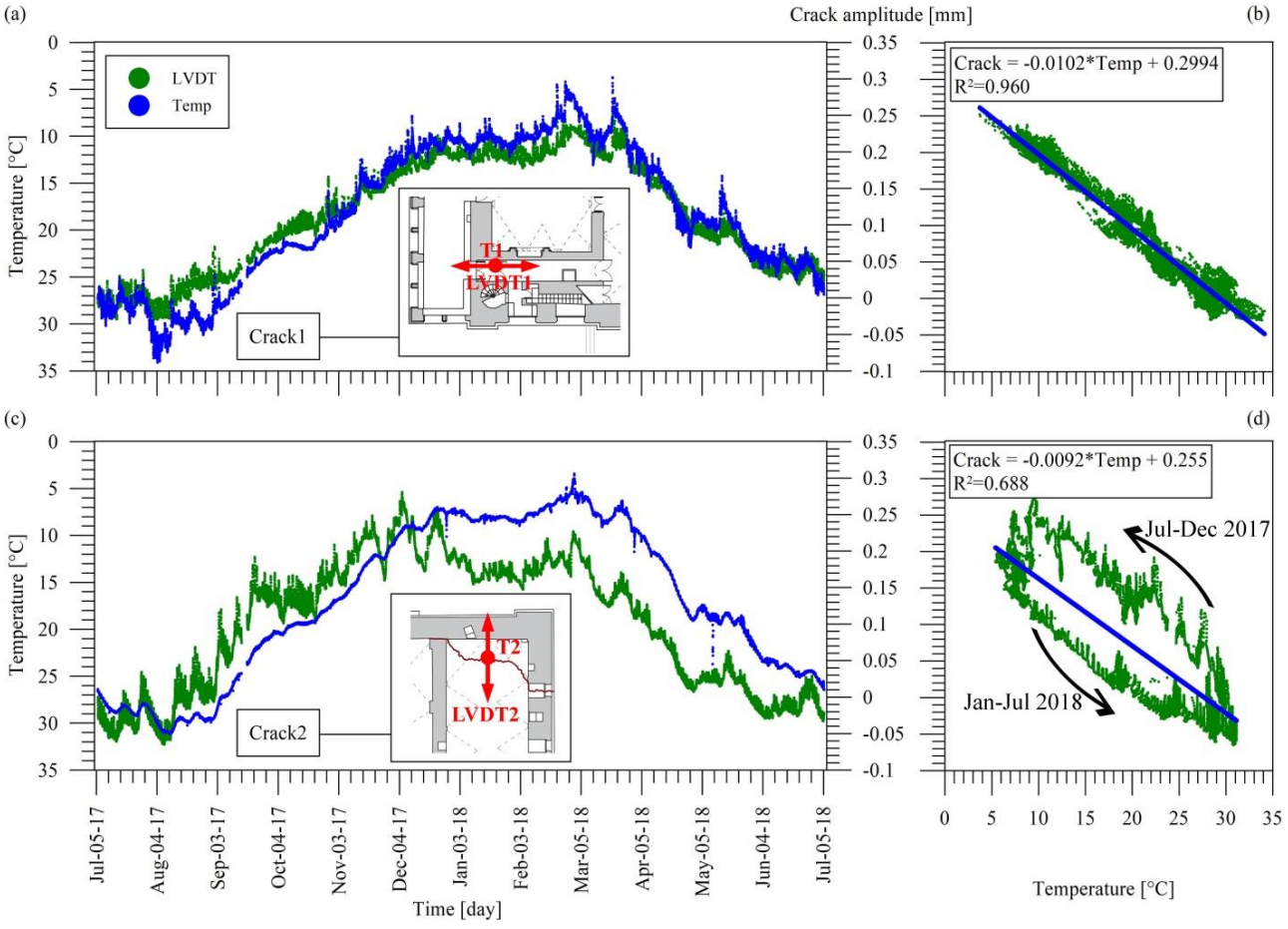

Fig. 10. Evolution in time of two monitored crack amplitudes and temperature data of Consoli Palace during the first year of monitoring and their correlation: LVDT1 and T1 (a), and LVDT2 and T2 (b).

An important temperature influence is also observed on dynamic signatures. In this regards, correlation coefficients between identified natural frequencies and temperature data are summarized in Table 6, consistently highlighting negative correlations. In particular, an overall large degree of negative temperature correlation is evidenced for modes Fy1, L1 and T1, which is also confirmed by the relatively high values of standard deviations and coefficients of variation (CVs) reported in Table 5 for the natural frequencies of such modes. The notable temperature effects affecting local mode L1 are clearly associated to the circumstance that the bell-tower is particularly exposed to the outdoor environment and to direct solar radiation. Considering the two global bending modes of vibration, Fx1 and Fy1, the higher degree of temperature correlation observed for mode Fy1 can be conceivably justified by noting that the two longitudinal

walls in North-South direction that are activated in mode Fy1 are under direct thermal effects with an externally exposed surface. On the contrary, half of the transversal walls in the East-West direction, activated in mode Fx1, are located indoor and, therefore, less exposed to temperature changes. Finally, the global torsional mode is especially influenced by the shear stiffness of the external walls of the Palace that are all directly exposed to outdoor temperature and to direct solar radiation.

Temperature-frequency correlation is further investigated in Figure 11 for modes Fx1, Fy1, L1 and T1. These results show that natural frequencies increase under decreasing temperature and that natural frequencies of modes Fy1 and L1 are almost overlapped to temperature data measured by sensor T1 taken with a negative sign. Temperature effects are also investigated in Figure 12, showing plots of all natural frequencies versus temperature data measured by sensor T1. Overall, an almost perfectly linear temperature correlation is observed for natural frequencies of modes Fy1, L1, L2 and T1, whereas frequency-temperature correlations of modes Fx1 and L3 are better represented by quadratic regression lines, highlighting more complicated temperature-driven mechanisms and, most likely, a more significant direct solar radiation effect, as well as the effects of thermal capacitance of the masonry.

The negative sign of the frequency-temperature correlation coefficients is especially noteworthy. In general, this trend is different from what observed in other long-term studies on masonry structures reported in the literature, such as civic and bell-towers, as well as churches, whereby increases in natural frequencies with increasing temperature were often documented. The positive correlation between modal frequencies and temperature is often explained as the effect of the rise in stiffness induced by closing of micro-cracks in mortar joints due to thermal expansion, as well as to a lower moisture content in the masonry. The Consoli Palace represents a quite different type of structure with respect to those investigated in the literature in a long-term monitoring perspective, characterized by a moderate state of structural damage and by various metallic reinforcements, such as the tie rods installed to reduce the lateral thrust of the majestic barrel vault of the Arengo hall. The observed decrease in natural frequencies due to temperature increases could be conceivably attributed to temperature-induced slackening of such metallic reinforcements, resulting in a global softening effect, that could be enhanced by the existing macro-cracking conditions.

The correlation between natural frequencies and temperature, as well as the correlation between crack amplitudes and temperature, result into a frequency-crack-amplitude correlation that is specifically studied in Table 6 and in Figure 13. Considering the approximately linear correlation between temperature T1 and amplitude of crack C1, plots of natural frequencies versus temperature T1 (negative trend) are essentially similar to plots of natural frequencies versus C1 crack amplitude (positive trend), therefore resembling linearity for modes Fy1, L1, L2 and T1, whereas exhibiting a high degree of nonlinearity for modes Fx1 and L3. A plot summarizing the mutual dependence of crack amplitudes and natural frequencies on temperature is shown in Figure 14.

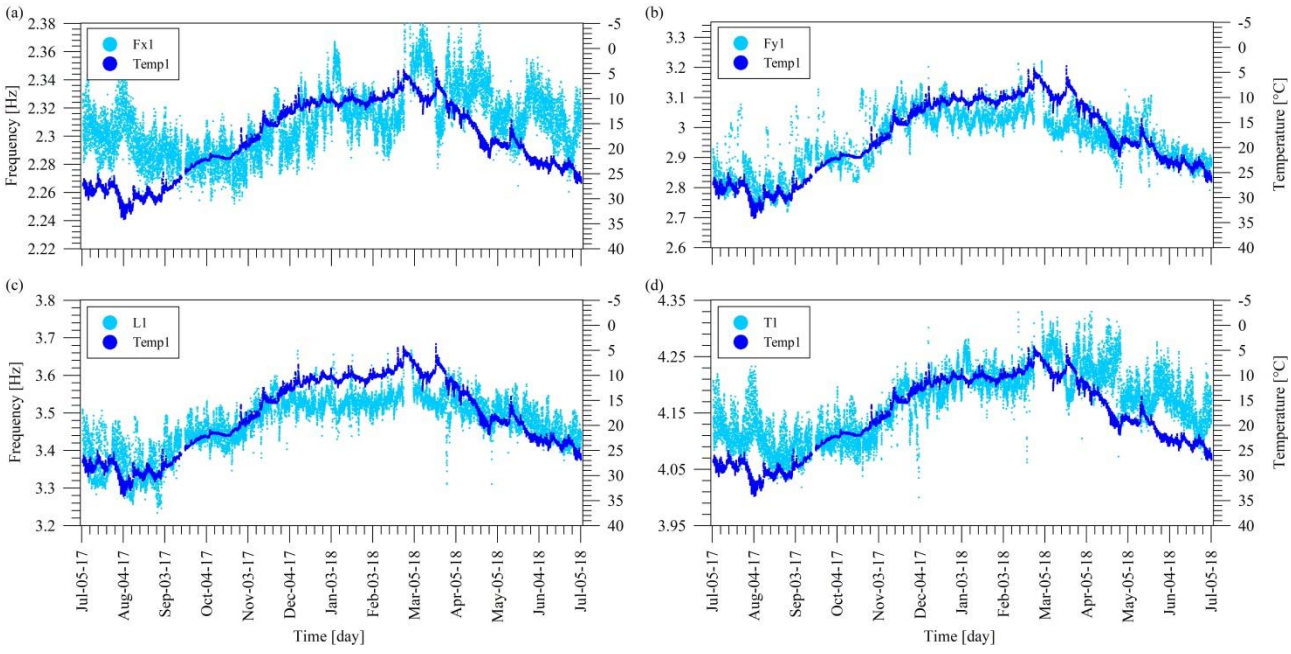

Fig. 11. Plots of time histories of most correlated natural frequencies and temperature data (T1): frequencies of modes Fx1 (a), Fy1 (b), L1 (c) and T1 (d).

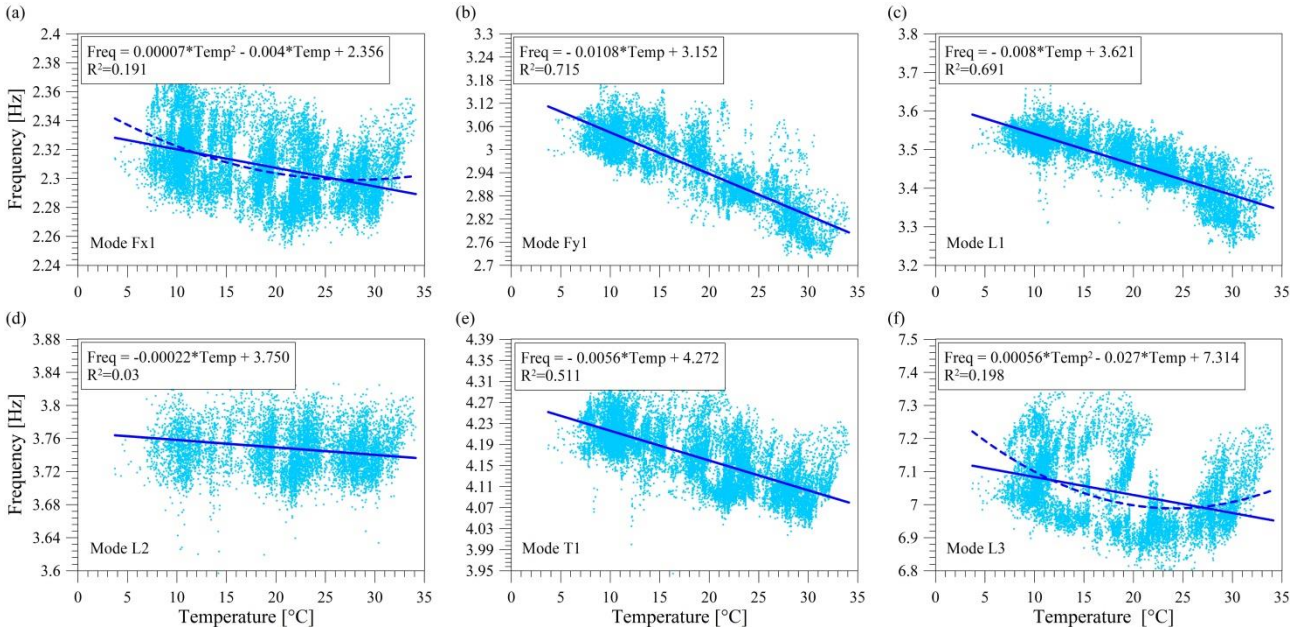

Fig. 12. Correlation between natural frequencies and temperature: plots of frequencies of modes Fx1 (a), Fy1 (b), L1 (c), L2 (d), T1 (e) and L3 (f) versus temperature data T1.

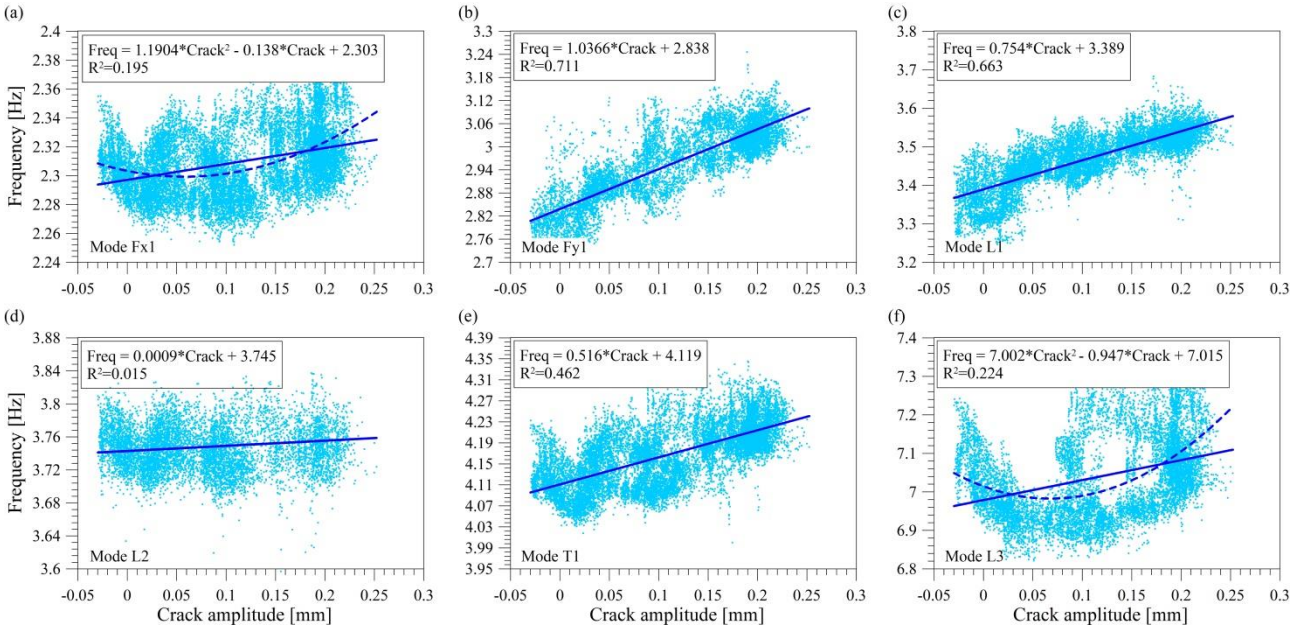

Fig. 13. Correlation between natural frequencies and crack amplitude: plots of frequencies of modes Fx1 (a), Fy1 (b), L1 (c), L2 (d), T1 (e) and L3 (f) versus crack amplitude C1.

4.4 Removal through MLR: statistical reconstruction of natural frequencies

The effects of changes in environmental conditions can be removed from identified natural frequency data using statistical techniques [24, 25, 26, 27]. For this purpose, multiple linear regressive (MLR) filters are often adopted, where linear correlations between a set of *r* dependent variables (natural frequencies) and a set of *p* independent variables (temperatures), called predictors, are exploited. In the present case, continuously tracked modal frequencies are the dependent variables, measured crack amplitudes can be regarded as either dependent or independent variables, while temperatures are independent variables. In general, dependent variables are stored in an observation matrix, **Y**, and their estimate, $\hat{\mathbf{Y}}$, can be written as

$$\hat{Y} = \boldsymbol{\beta}^T \boldsymbol{Z}^T \quad (3)$$

where matrix $\mathbf{Z} \in R^{N \times p+1}$ contains a first column of ones and *p* columns containing *N* values of the *p* selected independent

variables, while matrix $\boldsymbol{\beta} \in R^{p+1 \times r}$ contains constant terms in the first row and coefficients that weight the contribution of each independent variables in the remaining *p* rows.

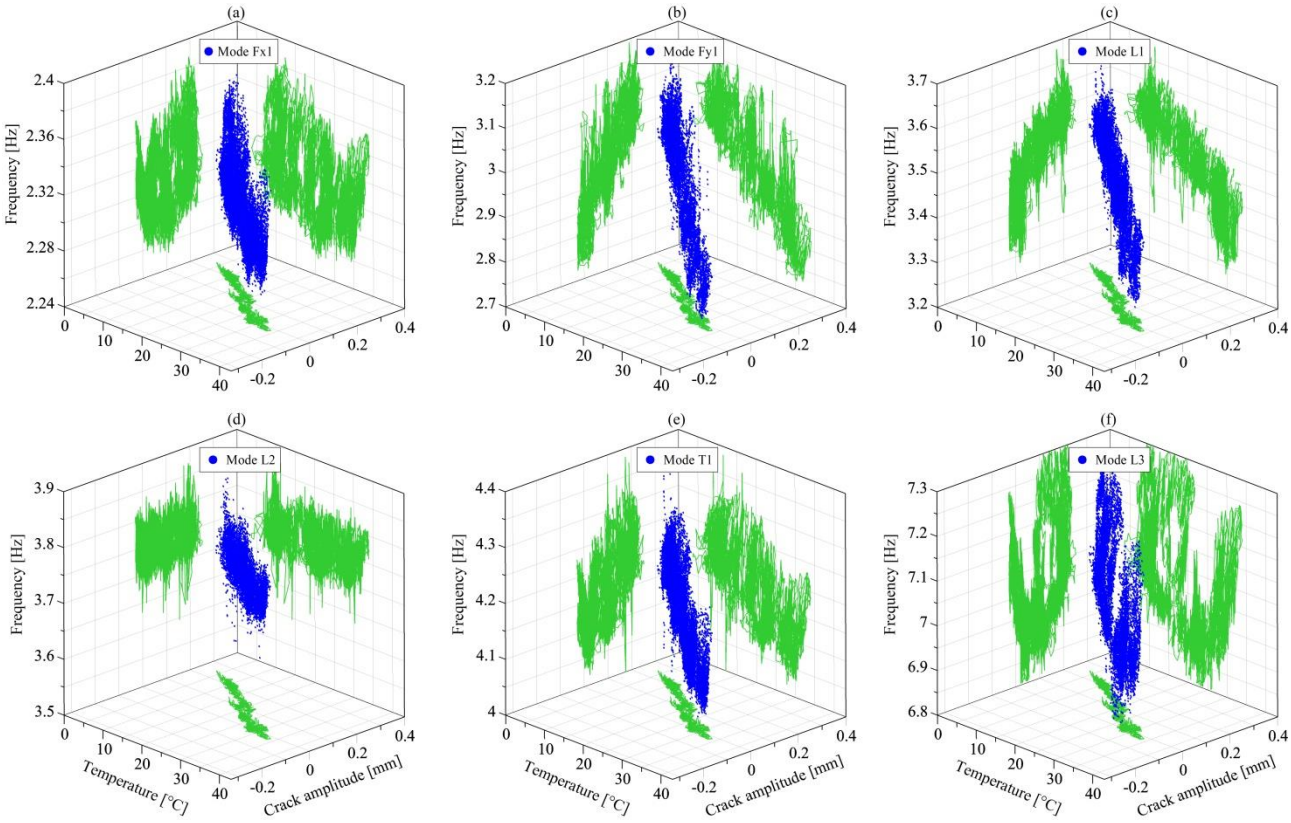

Fig. 14. Correlation between natural frequencies, 1st crack amplitudes and T1 temperature data during the monitoring period from July 5th 2017 to July 5th 2018.

The MLR model in Eq. (3) is referred to as "static" when independent and dependent variables are sampled at the same time, while it is referred to as "dynamic" when arrays of past observations of temperatures and/or crack amplitudes are used to construct a set of independent variables. In the context of the present paper, a dynamic model is found useful to catch delayed temperature-induced effects that might be caused by thermal inertia of the masonry and that might have originated the observed non-linear correlations between natural frequencies of some modes (Fx1 and L3 modes) and temperature.

The residual error matrix, **E**, between identified and predicted dependent variables is thus given by

$$\mathbf{E} = \mathrm{Y} - \boldsymbol{\beta}^T \boldsymbol{Z}^T \quad (4)$$

which represents the prediction error of the statistical model. The coefficients of the statistical model contained in matrix **β** are estimated in a least square sense by minimizing the norm of **E** in a reference training period. If the statistical model is successful in reproducing environmental effects on static or dynamic signatures, residuals in Eq. (4) are only minimally affected by changes in environmental conditions and therefore suitable to be used as damage sensitive features.

In order to show the effectiveness of MLR models for the problem under investigation, Figure 15 shows plots of the relative prediction errors of natural frequencies versus length of the training period. Three types of model are presented, namely: (i) a static model considering temperatures T1 and T2 as predictors (model Static_T), (ii) a dynamic model considering temperatures T1 and T2 at time *t*, *t*-6h, *t*-12h, *t*-24h and *t*-48h as predictors (model Dynamic_T) and (iii) a dynamic model considering temperatures T1 and T2 and crack amplitudes C1 and C2 at time *t*, *t*-6h, *t*-12h, *t*-24h and *t*-48h as predictors (model Dynamic_T_C). The results clearly highlight that the prediction error of the MLR models is almost minimized after about 4-5 months of training period length. Furthermore, the use of a dynamic model is seen to highly improve the quality of the prediction for the natural frequencies of mode Fx1 and L3, confirming that their non-linear correlations with respect to measured temperatures were due to delay effects associated with thermal inertia of the masonry. The advantage of including crack amplitudes as predictors is also quite evident in Figure 15, which is conceivably attributed to the role of the existing moderate damage state of the Palace. It is noteworthy to mention that introducing crack amplitudes as predictors, in addition to temperatures, for the statistical reconstruction of natural

frequencies time histories constitutes a novelty in the literature context, not observed in Structural Health Monitoring of historic masonry structures.

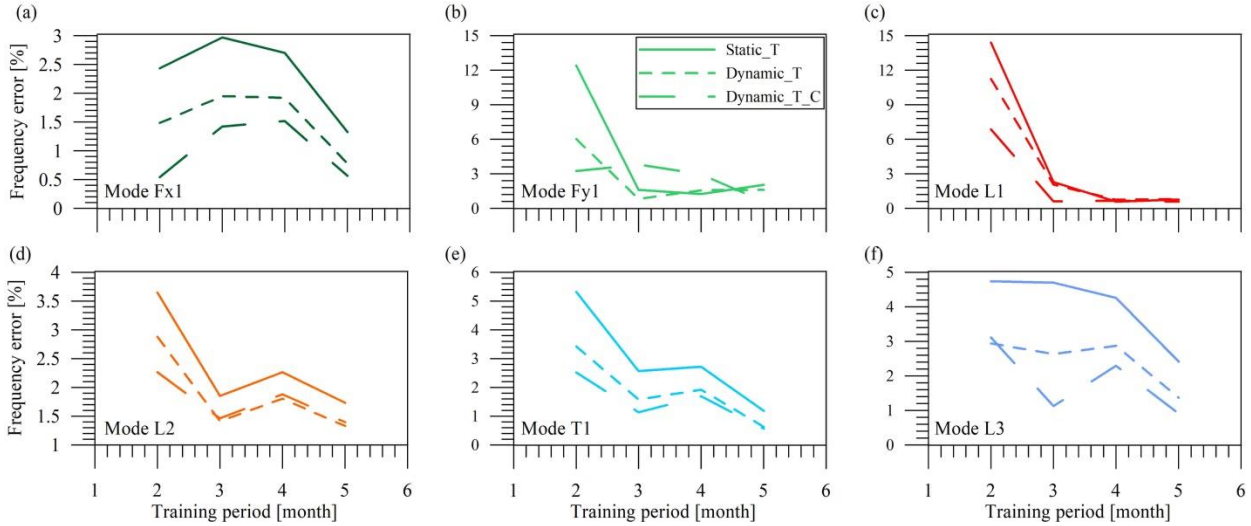

Fig. 15. Error between identified and predicted natural frequencies for increasing training period length: Fx1 (a), Fy1 (b), L1 (c), L2 (d), T1 (e) and L3 (f).

As examples demonstrating the quality of the MLR predictive models, Figure 16 shows time series of identified as well as predicted (using the model Dynamic_T_C) natural frequencies, considering a training period of 5 months (from July 5th to December 5th 2017). Overall, it is shown that dynamic MLR models are able to catch daily and longer term fluctuations in dependent variables, therefore being well suited to be used to remove temperature effects from monitoring data and to derive damage sensitive features.

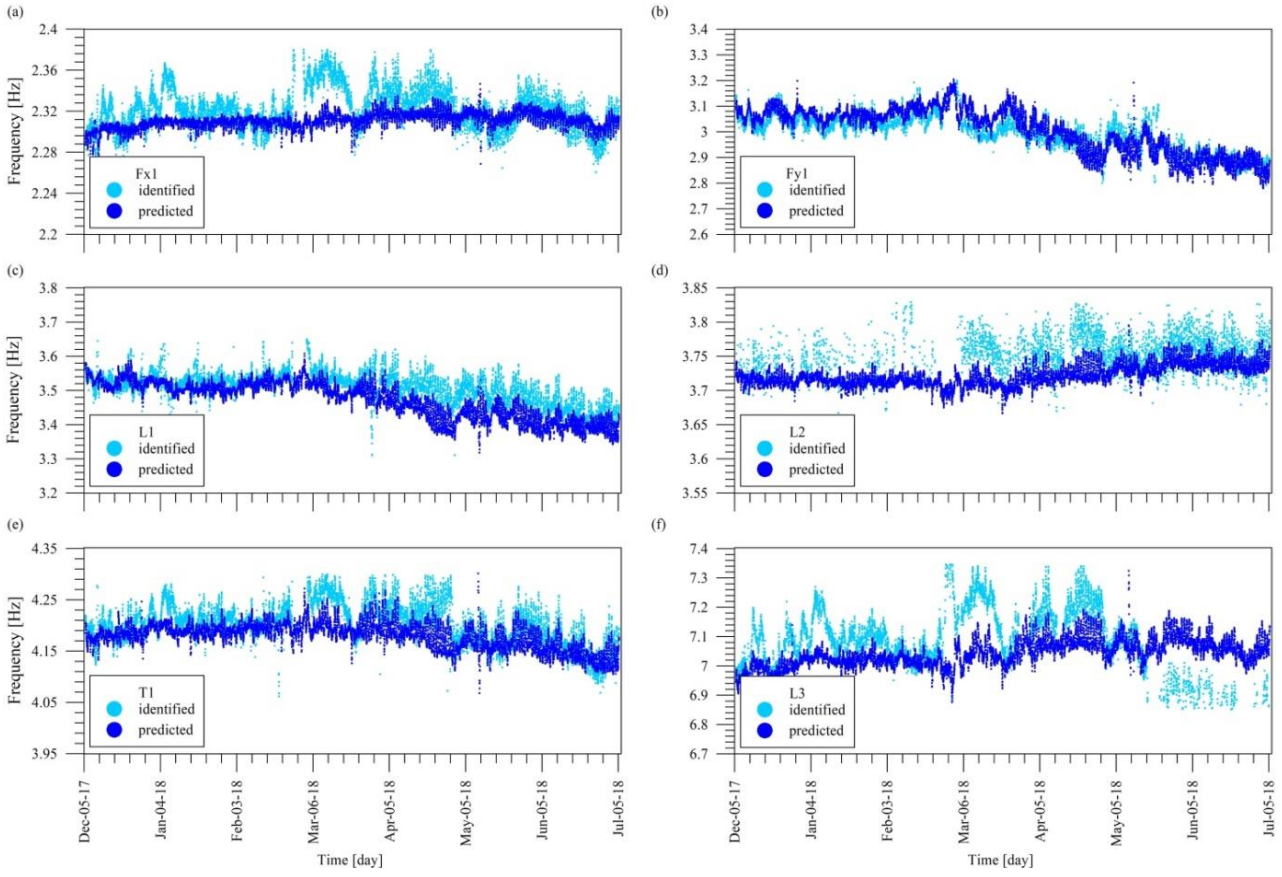

Fig. 16. Statistical reconstruction of natural frequencies in the monitoring period after 5 month of training period: Fx1 (a), Fy1 (b), L1 (c), L2 (d), T1 (e) and L3 (f).

4.5 Temperature effects: freezing conditions

The time period from February 25th to March 1st deserves a special attention because those were exceptionally cold days, when the air temperature in Gubbio remained constantly below 0 °C. Time series of natural frequencies tracked within such a monitoring period are shown in Figure 17, highlighting quite notable increases in all natural frequencies, which well agrees with other literature works on long-term monitoring of masonry structures [13, 14]. For reference purposes, the same Figure also reports the time history of air temperature recorded by an outdoor weather monitoring station located in the historical center of Gubbio. These results clearly show that increases in natural frequencies start as soon as air temperature decreases below 0°C, conceivably due to ice crystals forming in micro porosity of mortar joints and determining an overall stiffening effect, while natural frequencies start decreasing as soon as ice starts to melt. Natural frequencies reached their maximum values in about one day, conceivably after moisture in all pores with a sufficiently high degree of saturation was frozen, and, then, remained approximately constant for about 4 days until temperature raised again over 0°C. Afterwards, it took about two days for the natural frequencies to recover their initial values before freezing. As a side note, the effect of a possible splitting of the natural frequency of mode L2, already mentioned in Section 3, is also evidenced in Figure 17, but is not the focus of the present work. The same results of Figure 17 are presented in Figure 18 in terms of frequency-temperature plots. These plots clearly show the hysteresis associated to natural frequencies reaching this sort of plateau after about one day of freezing and to stiffening and softening effects caused by frost and thaw, respectively.

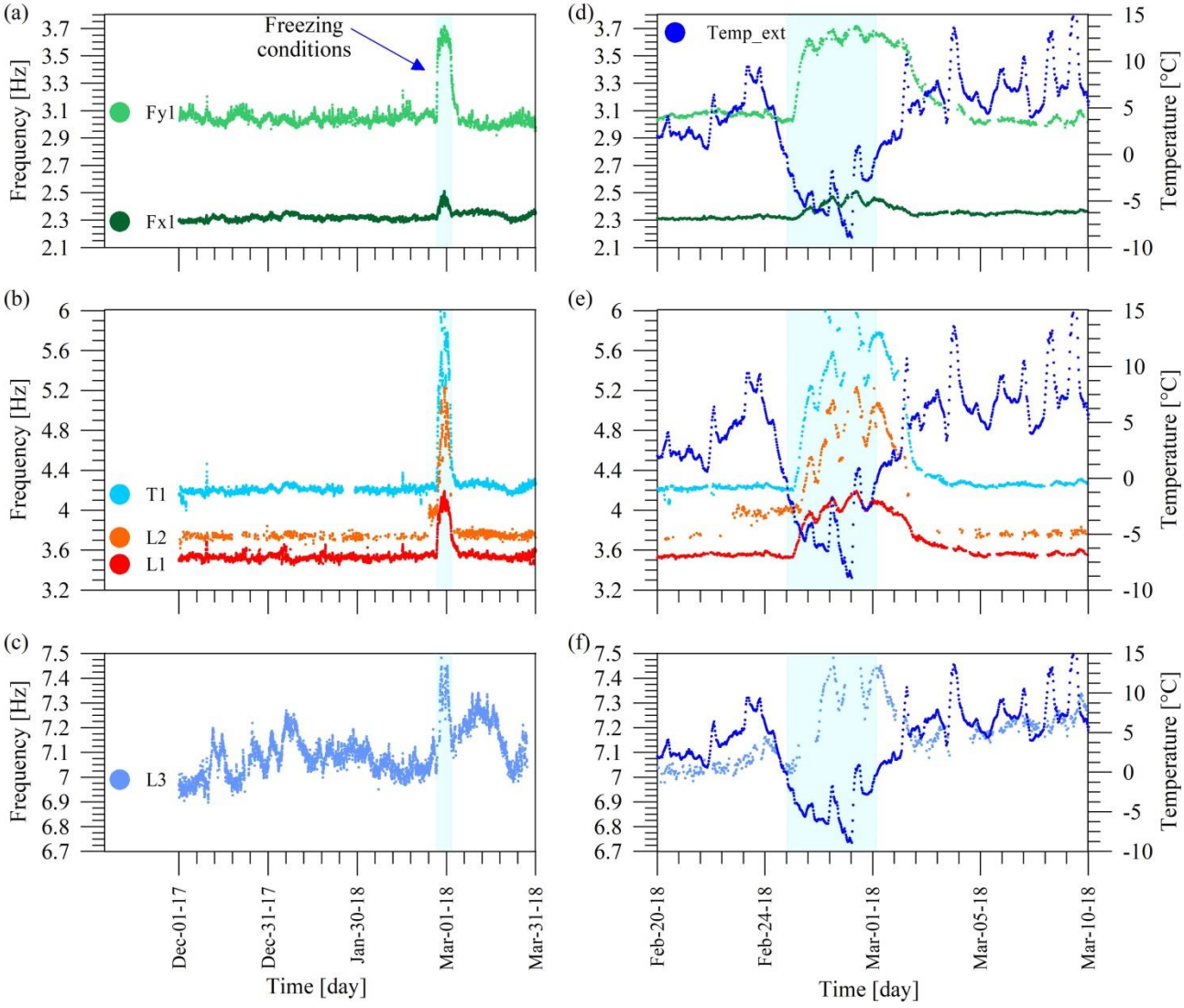

Fig. 17. Identified natural frequencies of Consoli Palace from December 1st 2017 with particular attention to freezing conditions occurred from February 25th to March 1st 2018: modes Fx1 and Fy1 (a), modes L1, L2 and T1 (b) and frequency of mode L3. Their zoom plots are shown in (d), (e) and (f), respectively.

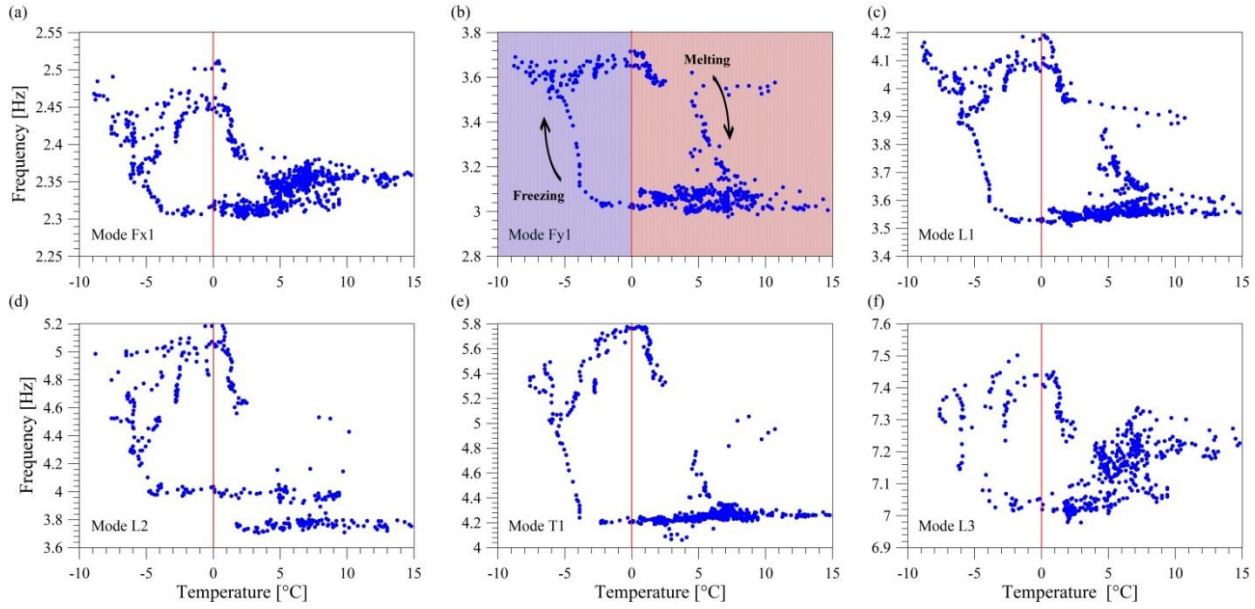

Fig. 18. Correlation in freezing conditions between natural frequencies and temperature: plots of frequencies of modes Fx1 (a), Fy1 (b), L1 (c), L2 (d), T1 (e) and L3 (f) versus external temperature data.

5. Conclusions

The paper has presented the analysis of the data recorded in the framework of the first year of activity of a simple low-cost mixed static and dynamic long-term SHM system installed by the authors on an iconic Italian monumental masonry palace: the Consoli Palace in Gubbio. This is the first example in the literature where continuous modal identification and SHM based on frequency tracking has been applied to the case of a stiff masonry palace, with the purpose of early detecting any damage or change in its structural behaviour following an earthquake or resulting from the effects of material degradation. The paper has been specifically focused on seasonal effects on the static and dynamic response of the structure, whose analysis and characterization is of pivotal importance in the SHM perspective. The main steps of the study and the major results achieved within the paper are listed below.

1. Geometrical and structural damage surveys have been carried out resulting in an accurate mapping of existing cracks within the Palace. Some of those cracks are compatible with the physiological cracking of a masonry building under dead loads, while other cracks are most likely associated to the effects of past earthquakes, such as the Umbria earthquake occurred on April 29th 1984, and may be associated to potential local failure mechanisms and, in particular, to a possible overturning of the loggia on the South façade and overturning of the northern part of West façade of the Palace due to the thrust of the vaults on the top of the building.
2. AVT and OMA, typically applied in the literature to slender structures, have revealed to be quite effective diagnostic tools also in the case of a monumental palace like the case study one. In particular, an AVT with two configuration setups was carried out on May 4th 2017 with excitation provided by microtremors, light wind and traffic, allowing identification of the first six modes of vibration within the range from 0 to 10 Hz. Natural frequencies, mode shapes and damping ratios of such modes have been consistently estimated by means of FDD, EFDD and SSI OMA techniques. Three of those modes of vibration involve vibration of the overall building, being two global flexural modes and one torsional mode, whereas the remaining three modes consist of mixed and/or local modes related to the dynamic interaction between the Palace and the bell-tower placed on its top.
3. A finite element elastic numerical model of the Palace has been developed and calibrated on the basis of experimentally identified modes of vibration, material properties (Young's modulus and Poisson's ratio) estimated by means of direct and indirect sonic tests and a direct manual tuning based on first order modal sensitivity analysis. A very good agreement has been achieved between the numerical model and the identified modal properties of the structure, allowing to conclude that all structural modes comprised in the frequency range of interest have been correctly identified.
4. Overall, damage survey, AVT and numerical modeling have provided the necessary information for the conceptual development and installation of the long-term SHM system, consisting of two crack meter sensors, two surface temperature sensors, and three high sensitivity accelerometers to track the evolution of modal properties of the structure. Application of an SSI-data automated modal analysis procedure developed by the authors in previous work to the first year of monitoring data has allowed to effectively track the evolution in time of the natural frequencies and damping ratios of the six identified modes of the Palace, which represents a novelty in the literature in the context of long-term monitoring of stiff masonry buildings such as palaces, whereby previous applications of modal tracking to masonry structures were essentially limited to slender towers.

5. Significant thermal effects on both crack amplitudes and natural frequencies of the Consoli Palace have been highlighted, whose removal represents a key step towards an effective use of this information for damage detection. Overall, correlations between crack amplitudes and temperature have proved to be almost linear, while correlations between natural frequencies and temperature are sometimes non-linear. This effect has been attributed to thermal inertia of the masonry resulting in a time shift between changes in air temperature and changes in natural frequencies. This is confirmed by the circumstance that dynamic multivariate linear regression models, using past values of predictors, have proved quite effective for removing temperature effects from identified natural frequencies. Furthermore, the use of crack amplitudes as predictors allowed to improve statistical modeling of natural frequencies, which is important in the SHM perspective.
6. A negative correlation between surface masonry temperature and crack amplitudes has been evidenced which is conceivably associated to temperature-induced volume variations: the global contraction/dilatation of structural masonry volumes results in opening/closing of pass-through cracks.
7. A very important result of this work regards the natural frequencies variations with changes in ambient temperature. Differently from what observed in other literature works on vibration-based monitoring of masonry buildings, an unexpected negative correlation between natural frequencies and temperature has been found for the Consoli Palace. This negative correlation is indeed observed for the first time, with respect to positive natural frequencies-temperature correlations of masonry structures such as slender towers and stiffer structures such as churches and/or cathedrals. The marked increase in natural frequencies of global vibration modes of the Palace with decreasing ambient temperature has been attributed to an increase in global structural stiffness due to strengthening effects of metallic reinforcements (tie rods shortening at lower temperatures) and the presence of a moderate structural damage state in the Palace.
8. As already known from other literature works on slender masonry structures, such as civic and bell-towers, correlations between natural frequencies and temperature change dramatically in freezing conditions. During some exceptional cold days between February and March 2018 remarkable freezing effects on natural frequencies have been observed also for the Consoli Palace. During those days, when temperature was constantly below 0 °C, natural frequencies exhibited sharp increases, conceivably caused by the stiffening effect produced by ice crystals forming within the micro-pores of the masonry.

Overall, the presented results show a promise towards the application of long-term vibration-based SHM to masonry palaces like the Consoli Palace. Of particular interest are the use of crack amplitudes as predictors in statistical modelling of time series of natural frequencies and the relationship between natural frequencies and temperature, which has an opposite sign if compared to what observed in other literature works on SHM of masonry buildings and that could be the result of the existing moderate damage state of the building.

Acknowledgements

This project has received funding from the European Union's Framework Programme for Research and Innovation HORIZON 2020 under grant agreement No 700395.

The authors gratefully acknowledge Professors Paulo B. Lourenço and Luís F. Ramos (University of Minho, Portugal), and Dr. Pier Francesco Giordano (Politecnico di Milano, Italy), for their valuable advices regarding the execution of sonic tests.

References

[1] L. Luzi, F. Pacor, G. Ameri, R. Puglia, P. Burrato, M. Massa, P. Augliera, G. Franceschina, S. Lovati, R. Castro, Overview on the strong-motion data recorded during the May–June 2012 Emilia seismic sequence. Seismol Res Lett 84(4): (2013) 629–644.

[2] ReLUIS-INGV Workgroup (2016) Preliminary study on strong motion data of the 2016 central Italy seismic sequence V6. http:// www.reluis.it.

[3] F. Magalhães, A. Cunha, E. Caetano, Online automatic identification of the modal parameters of a long span arch bridge, Mech. Syst. Signal Process. 23 (2009) 316–329.

[4] C. Rainieri, G. Fabbrocino, Automated output-only dynamic identification of civil engineering structures, Mech. Syst. Signal Process. 24 (2010) 678–695.

[5] F. Ubertini, C. Gentile, A.L. Materazzi, Automated modal identification in operational conditions and its application to bridges, Eng. Struct. 46 (2013) 264–278.

[6] E. Reynders, J. Houbrechts, G. De Roeck, Fully automated (operational) modal analysis. Mech. Syst. Signal Process. 29: (2012) 228–250.

[7] A. Cabboi, F. Magalhães, C. Gentile, A. Cunha, Automated modal identification and tracking: application to an iron arch bridge. Struct Control Health Monit 24(2017):e1854.

[8] R. Cardoso, A. Cury, F. Barbosa, A robust methodology for modal parameters estimation applied to SHM. Mech Syst Signal Pr (2017) 95:24–41.
[9] F. Clementi, A. Pierdicca, A. Formisano, F. Catinari, S. Lenci, Numerical model upgrading of a historical masonry building damaged during the 2016 Italian earthquakes: the case study of the Podestà palace in Montelupone (Italy) Journal of Civil Structural Health Monitoring, (2017) 7 (5), pp. 703-717.
[10] R. Cantieni, One-year monitoring of a historic bell tower. In: Proceedings of the 9th international conference on structural dynamics (EURODYN 2014), Porto, Portugal (2014), pp. 1493–1500
[11] F. Ubertini, N. Cavalagli, A. Kita, G. Comanducci, Assessment of a monumental masonry bell-tower after 2016 Central Italy seismic sequence by long-term SHM. Bull of Earthquake Eng (2018), 16:775-801.
[12] C. Liu, Y. Gong, S. Laflamme, B. Phares, S. Sarkar, Bridge damage detection using spatiotemporal patterns extracted from dense sensor network, Measurement Science and Technology, 28(1), 2017, Art. N. 014011.
[13] F. Ubertini, G. Comanducci, N. Cavalagli, A.L. Pisello, A.L. Materazzi, F. Cotana, Environmental effects on natural frequencies of the San Pietro bell tower in Perugia, Italy and their removal for structural performance assessment. Mech. Syst. Signal Process. 82: (2017) 307–322.
[14] C. Gentile, M. Guidobaldi, A. Saisi, One-year dynamic monitoring of a historic tower: damage detection under changing environment. Meccanica 51: (2016) 2873–2889.
[15] F. Magalhães, A. Cunha, E. Caetano, Vibration based structural health monitoring of an arch bridge: from automated OMA to damage detection, Mech. Syst. Signal Process. 28 (2012) 212–228.
[16] A. Cabboi, C. Gentile, A. Saisi, From continuous vibration monitoring to FEM-based damage assessment: Application on a stone-masonry tower, Construction and Building Materials, 156, (2017), pp. 252-265.
[17] N. Cavalagli, M. Gioffrè, V. Gusella, Structural monitoring of monumental buildings: The Basilica of Santa Maria Degli Angeli in Assisi (ITALY) COMPDYN 2015 - 5th ECCOMAS Thematic Conference on Computational Methods in Structural Dynamics and Earthquake Engineering, (2015) pp. 2410-2422.
[18] A. De Stefano, E. Matta, P. Clemente, Structural health monitoring of historical heritage in Italy: some relevant experiences, Journal of Civil Structural Health Monitoring, 6 (1), (2016) pp. 83-106.
[19] V. Gattulli, M. Lepidi, F. Potenza, Dynamic testing and health monitoring of historic and modern civil structures in Italy, Structural Monitoring and Maintenance, 3 (1), (2016) pp. 71-90.
[20] A. Cigada, L. Corradi Dell'Acqua, B. Mörlin Visconti Castiglione, M. Scaccabarozzi, M. Vanali, E. Zappa, Structural Health Monitoring of an Historical Building: The Main Spire of the Duomo Di Milano, International Journal of Architectural Heritage, 11 (4), (2017) pp. 501-518.
[21] F. Potenza, F. Federici, M. Lepidi, V. Gattulli, F. Graziosi, A. Colarieti, Long-term structural monitoring of the damaged Basilica S. Maria di Collemaggio through a low-cost wireless sensor network, Journal of Civil Structural Health Monitoring, 5 (5), (2015) pp. 655-676.
[22] E. Mesquita, F. Brandão, A. Diogenes, P. Antunes, H. Varum, Ambient vibrational characterization of the Nossa Senhora das Dores Church, Engineering Structures and Technologies, 9:4, (2017) 170-182.
[23] J. Noh, S. Russo, Long-term dynamic monitoring of the historical masonry façade: the case of Palazzo Ducale in Venice, Italy, ISPRS Ann. Photogramm, Remote Sens. Spatial Inf. Sci., IV-2/W2, (2017), 187-193.
[24] P.P. Rossi, C. Rossi, Monitoring of Two Great Venetian Cathedrals: San Marco and Santa Maria Gloriosa Dei Frari, International Journal of Architectural Heritage, 9 (1), (2015) pp. 58-81.
[25] L. B. Benatov Vega, F. Sánchez Domínguez, I. Poy López, The monitoring of Barcelona's Sagrada Familia church with fiber optic technology. control of the construction of a nearby tunnel. SHMII-5 2011 - 5th International Conference on Structural Health Monitoring of Intelligent Infrastructure, (2011) 10 p.
[26] M.G. Masciotta, L.F. Ramos, P.B. Lourenço, J.A.C. Matos, Development of key performance indicators for the structural assessment of heritage buildings, 8th European Workshop on Structural Health Monitoring, EWSHM 2016, 1, pp. 606 617.
[27] S. Russo, On the monitoring of historic Anime Sante church damaged by earthquake in L'Aquila, Structural Control and Health Monitoring, 20 (9), (2013) pp. 1226-1239.
[28] I. Lombillo, H. Blanco, J. Pereda, L. Villegas, C. Carrasco, J. Balbás, Structural health monitoring of a damaged church: design of an integrated platform of electronic instrumentation, data acquisition and client/server software, Journal of Structural Control and Health Monitoring. 23, (2016) 69–81.
[29] F. Marazzi, P. Tagliabue, F.M. Corbani, Traditional vs innovative structural health monitoring of monumental structures: A case study, Struct. Control Health Monitoring, 18, (2011) 430-449.
[30] F. Lorenzoni, F. Casarin, M. Caldon, K. Islami, C. Modena, Uncertainty quantification in structural health monitoring: Applications on cultural heritage buildings. Mech. Syst. Signal Process., 66– 67 (2016):268–281.

[31] F. Ottoni, C. Blasi, Results of a 60-Year Monitoring System for Santa Maria del Fiore Dome in Florence, International Journal of Architectural Heritage, 9 (2014):1, 7-24.
[32] R. Ceravolo, A. De Marinis, M.L. Pecorelli, L. Zanotti Fragonara, Monitoring of masonry historical constructions: 10 years of static monitoring of the world's largest oval dome. Struct Control Health Monit. 2017;24:e1988.
[33] M.A. Chiorino, C. Calderini, A. Spadafora, R. Spadavecchia, Structural assessment, testing, rehabilitation and monitoring strategies for the world's largest elliptical dome and sanctuary of Vicoforte, SacoMatis 2008, International RILEM Conference.
[34] H. Sohn, Effects of environmental and operational variability on structural health monitoring. Philos Trans R Soc A 365: (2007)539–560.
[35] L.F. Ramos, L. Marques, P.B. Lourenço, G. DeRoeck, A. Campos-Costa, J.C.A. Roque, Monitoring historical masonry structures with operational modal analysis: two case studies. Mech. Syst. Signal Process. 24(5): (2010) 1291–1305.
[36] A. Saisi, C. Gentile, Post-earthquake diagnostic investigation of a historic masonry tower. Journal of Cultural Heritage, 16(4), 2015, 602–609.
[37] A. Saisi, C. Gentile, M. Guidobaldi, Post-earthquake continuous dynamic monitoring of the Gabbia Tower in Mantua, Italy, Constr. Build. Mater. 81 (2015) 101–112.
[38] M.G. Masciotta, J.C.A. Roque, L.F. Ramos, P.B. Lourenço, A multidisciplinary approach to assess the health state of heritage structures: The case study of the Church of Monastery of Jerónimos in Lisbon, Construction and Building Materials, 116, (2016) pp. 169-187.
[39] M.G. Masciotta, L.F. Ramos, P.B. Lourenço, The importance of structural monitoring as a diagnosis and control tool in the restoration process of heritage structures: A case study in Portugal, Journal of Cultural Heritage, 27, (2017) pp. 36-47.
[40] A. Elyamani, O. Caselles, P. Roca, J. Clapes, Dynamic investigation of a large historical cathedral, Structural Control and Health Monitoring, 24 (3), (2017) art. no. e1885.
[41] S. Wenchen, W. Xianqiang, J Yubo, Modeling of Temperature Effect on Modal Frequency of Concrete Beam Based on Field Monitoring Data, Shock and Vibration, vol. 2018, Article ID 8072843, 13 pages, 2018.
[42] Y. Xia, B. Chen, S. Weng, Y.-Q. Ni, and Y.-L. Xu, Temperature effect on vibration properties of civil structures: a literature review and case studies, Journal of Civil Structural Health Monitoring, (2012) 2:29–46.
[43] F. Lorenzoni, F. Casarin, C. Modena, M. Caldon, K. Islami, F. da Porto, Structural health monitoring of the Roman Arena of Verona, Italy, Journal of Civil Structural Health Monitoring, 3 (4), (2013) pp. 227-246.
[44] A. Saisi, C. Gentile, A. Ruccolo, Continuous monitoring of a challenging heritage tower in Monza, Italy, Journal of Civil Structural Health Monitoring, 8 (1), (2018) pp. 77-90.
[45] L. Binda, M. Falco, C. Poggi, A. Zasso, R.G. Mirabella, R. Corradi, R. Tongini Folli, Static and dynamic studies on the Torrazzo in Cremona(Italy): the highest masonry bell tower in Europe, Proc. of the IASS-MSU International Symposium "Bridging large spans: from antiquity to the present", Istanbul, (2000), 100-110.
[46] D. Uglešić, U. Bohinc, Monitoring of cracks on the bell tower of St. Anastasia cathedral in Zadar Croatia, EWSHM - 7th European Workshop on Structural Health Monitoring, Jul 2014, Nantes, France. 2014.
[47] K. Worden, H. Sohn, C. Farrar, Novelty detection in a changing environment: regression and interpolation approaches, J. Sound Vib. 258 (2002) 741–761.
[48] A. Yan, G. Kerschen, P. De Boe, J. Golinval, Structural damage diagnosis under varying environmental conditions part i: a linear analysis, Mech. Syst. Signal Process. 19 (2005) 847–864.
[49] A. Yan, G. Kerschen, P. De Boe, J. Golinval, Structural damage diagnosis under varying environmental conditions part ii: local PCA for non-linear cases, Mech. Syst. Signal Process. 19 (2005) 865–880.
[50] A. Bellino, A. Fasana, L. Garibaldi, S. Marchesiello, PCA-based detection of damage in time-varying systems, Mech. Syst. Signal Process. 24 (2010) 2250–2260.
[51] A. Mosavi, D. Dickey, R. Seracino, S. Rizkalla, Identifying damage locations under ambient vibrations utilizing vector autoregressive models and Mahalanobis distances, Mech. Syst. Signal Process.(2012) 254–267.
[52] G. Comanducci, F. Ubertini, A. Materazzi, Structural health monitoring of suspension bridges with features affected by changing wind speed, J. Wind Eng. Ind. Aerodyn. 141 (2015) 12–26.
[53] F. Ubertini, G. Comanducci, N. Cavalagli, Vibration based structural health monitoring of a historic bell-tower using output-only measurements and multivariate statistical analysis, Structural Health Monitoring, 15(4), (2016) 438-457.

[54] A. Alvandi, C. Cremona, Assessment of vibration-based damage identification techniques, J. Sound Vib. 292 (2006) 179–202.
[55] A.L. Materazzi, F. Ubertini, Eigenproperties of suspension bridges with damage, J. Sound Vib. 330 (2011) 6420–6434.
[56] C. Farrar, K. Worden, An introduction to structural health monitoring, Philos. Trans. R. Soc. 365 (2007), 303–315.
[57] J. Wu, C. Song, H.S. Saleem, A. Downey, S. Laflamme, Network of flexible capacitive strain gauges for the reconstruction of surface strain, Measurement Science and Technology, (2015) Volume 26, Issue 5, 1 May 2015, Article number 055103, Pages 1-12.
[58] A. Downey, C. Hu, S. Laflamme, Optimal sensor placement within a hybrid dense sensor network using an adaptive genetic algorithm with learning gene pool, Structural Health Monitoring, in press, 2018.
[59] F. Aras, L. Krstevska, G. Altay, L. Tashkov, Experimental and numerical modal analyses of a historical masonry palace, Construction and Building Materials, (2011) 25:81-91.
[60] G.P. Cimellaro, A. De Stefano, Ambient vibration tests of XV century Renaissance Palace after 2012 Emilia earthquake in Northern Italy, Structural Monitoring and Maintenance, (2014), 1:231-247.
[61] A. Formisano, L. Krstevska, G. Di Lorenzo, R. Landolfo, L. Tashkov, Experimental ambient vibration tests and numerical investigation on the Sidoni Palace in Castelnuovo of San Pio (L'Aquila, Italy), Int. J. of Masonry Research and Innovation, (2018), 3:269 – 294.
[62] F. Lorenzoni, M. Caldon, F. da Porto, C. Modena, T. Aoki, Post-earthquake controls and damage detection through structural health monitoring: applications in l'Aquila, J Civil Struct Health Monit (2018) 8: 217-236.
[63] H. Haessler, R. Gaulon, L. Rivera, R. Console, M. Frongneux, G. Gasparini, L. Martel, G. Patau, M. Siciliano, A. Cisternas, The Perugia (Italy) earthquake of 29, April 1984: a micro-earthquake survey. Bulletin Seismological Society of America 78, 1988, 1948–1964.
[64] G. Ameri, F. Gallovič, F. Pacor, A. Emolo, Uncertainties in strong ground-motion prediction with finite-fault synthetic seismograms: An application to the 1984 M 5.7 Gubbio, central Italy, earthquake (2009) Bulletin of the Seismological Society of America, 99 (2 A), pp. 647-663.
[65] I. Catapano, G. Ludeno, F. Soldovieri, F. Tosti, G. Padeletti, Structural Assessment via Ground Penetrating Radar at the Consoli Palace of Gubbio (Italy). Remote Sens. 2018, 10, 45.
[66] R. Brincker, L.M. Zhang, P. Andersen, Modal identification from output-only systems using frequency domain decomposition, Smart Materials & Structures, 10, 2001, 441-445.
[67] SVS, ARTeMIS Extractor 2010 release 5.0., http://www.svibs.com/, 2010.
[68] N. Cavalagli, V. Gusella, Dome of the basilica of Santa Maria degli Angeli in Assisi: Static and dynamic assessment, International Journal of Architectural Heritage, 9 (2), (2015) pp. 157-175.
[69] M. Valente, G. Milani, Seismic assessment of historical masonry towers by means of simplified approaches and standard (FEM), Construction and Building Materials, 108, (2016) 74 – 104.
[70] F. Clementi, V. Gazzani, M. Poiani, P.A. Mezzapelle, S. Lenci, Seismic assessment of a monumental building through nonlinear analysis of a 3D solid model, Journal of Earthquake Engineering, in press, (2017).
[71] J. Lubliner, J. Oliver, S. Oller, E. Oñate, A Plastic-Damage Model for Concrete, International Journal of Solids and Structures, 25(3), (1989) 229–326.
[72] J. Lee, G. Fenves, Plastic-Damage Model for Cyclic Loading of Concrete Structures, Journal of Engineering Mechanics, 124, (1989) 892–900.
[73] NTC08 (2008), Norme Tecniche per le Costruzioni (Italian). Italian Ministry of Infrastructures and Transport.
[74] D. McCann, M. Forde, Review of NDT methods in the assessment of concrete and masonry structures, NDT&E International, vol. 34, (2001) pp. 71-84.
[75] E. Manning, L.F. Ramos, F. Fernandes, Direct Sonic and Ultrasonic Wave Velocity in Masonry under Compressive Stress, 9th International Masonry Conference, Guimarães, 2014.
[76] National Instruments Corporation. LabVIEW user manual. Austin, TX: National Instruments Corporation, 2003.